AD _____

TECHNICAL REPORT ECOM-02071-1

INVESTIGATION OF THE QUANTITATIVE DETERMINATION OF PRECIPITATION BY RADAR

INTERIM REPORT NO. 1

by

E. A. Mueller - A. L. Sims - R. Cataneo

June 1967

ECOM

ATMOSPHERIC SCIENCES LABORATORY
UNITED STATES ARMY ELECTRONICS COMMAND • FORT MONMOUTH, N.J.

Contract DA-28-043 AMC-02071(E)
ILLINOIS STATE WATER SURVEY
at the
University of Illinois
Urbana, Illinois

NOTICES

Disclaimers

The findings in this report are not to be construed as an official Department of the Army position, unless so designated by other authorized documents.

The citation of trade names and names of manufacturers in this report is not to be construed as official Government indorsement or approval of commercial products or services referenced herein.

Disposition

Destroy this report when it is no longer needed. Do not return it to the originator.

TECHNICAL REPORT ECOM-02071-1 June 1967

INVESTIGATION OF THE QUANTITATIVE DETERMINATION OF PRECIPITATION BY RADAR

INTERIM REPORT NO. 1

1 October 1966 to 31 March 1967

Contract No. DA-28-043 AMC-02071(E)
DA Project No. 1V0-14501-B-53A-07

Prepared by

E. A. Mueller, A. L. Sims, and R. Cataneo

ILLINOIS STATE WATER SURVEY
at the
University of Illinois
Urbana, Illinois

for

ATMOSPHERIC SCIENCES LABORATORY

U. S. ARMY ELECTRONICS COMMAND, FORT MONMOUTH, N. J.

ABSTRACT

The results of a study of the measurement of rainfall by radar at a range of 75 miles are presented. Some of the problems of radar measurements at this range are found to be attenuation and effects of the radar beam's large vertical extent at distant ranges.

The analysis of drop-size data from rains at Flagstaff, Arizona shows that the radar-rainfall relationships there are quite different from those measured elsewhere by the drop camera technique.

Results of a study of drop-size distributions from New Jersey and North Carolina are presented. In many respects, the data from these two locations are similar.

A paper dealing with the analysis of drop-size data from Florida and Oregon is included as an appendix.

CONTENTS

RADAR MEASUREMENT OF RAIN USING THE KANKAKEE NETWORK

In order to evaluate the usefulness of radar to measure rainfall at more distant ranges, the Kankakee Raingage Network was established near Kankakee, Illinois in the spring of 1966. This network is located at a mean range of 65.5 nautical miles from the CPS-9 radar at Champaign. It consists of 16 recording gages spaced in a nearly square grid of 4 rows, each row having 4 gages. The network area is approximately 400 square miles. More detailed description of this network is contained in Technical Report EC0M-00032-F.

Data

The Kankakee network was operated from April 15 to September 30, 1966. Forty-one sets of raingage charts were obtained during this period. The 24-hour charts used were generally changed twice weekly.

The CPS-9 radar was operated to record as much of the rain over the network as possible with the limited staff. Step-gain scope photographs were made at 4- or 8-minute intervals. A nominal elevation angle of 0 degrees and a range of 100 miles were used.

Originally, 15 storms were chosen for analysis on the basis of having at least one gage with 0.05 inch or more of rain and having at least 30-minutes of concurrent radar and gage data. Two of these storms have been eliminated because of data deficiencies discovered as the analysis proceeded. Two other storms occurring on the same day have been combined into a single storm.

The gage data for the storms studied are on 14 sets of charts. The information on these charts was converted to punch cards by means of a Benson Lehner "Oscar" chart reader. These cards were processed by a computer program which produced a listing of 15-minute amounts for each gage. These amounts were then combined to obtain 30-minute amounts, which were used to calculate mean network amounts for each 30-minute period and for each storm.

Radar-Rainfall Analysis

The radar data analysis began with the tracing of the echoes onto paper. For this purpose, the radar film was projected to a scale of 3 mm per mile, making the network a 6-cm square on the tracings. The network area was then drawn on the tracing paper along with the iso-echo contours.

Using a planimeter, the fraction of the network covered by echo was determined for each gain step in each series. The measurements for each series within each 30-minute period were combined by averaging areas, weighting each area by the time period it represented, usually 4 minutes. This gave a 30-minute average area for each step.

An appropriate rainfall rate was determined for each gain step level from the radar equation, a Z-R relationship, and the radar calibration data. The radar equation derived by Probert-Jones[1] was used. By substituting in this equation the parameters of the CPS-9 radar and a range of 65.5 nautical miles, the radar equation was reduced to the following form:

$$P_r/P_t = 2.94 \times 10^{-20} Z$$

where Z is the radar reflectivity in $mm^6\ m^{-3}$. The transmitted power, P_t, was measured frequently during the data collection season. Also, measurements of the minimum discernible received power, P_r, was measured for each step using a known calibrating signal. From these calibration measurements, a minimum discernible Z was determined for each step level and each storm date. The sensitivity of the radar was low during the early part of the season, but was improved to near normal sensitivity by August and September.

To convert Z to rainfall rate, R, the following relationships were used, depending upon the type of rain which was predominant during the storm:

Thunderstorms	$Z = 435R^{1.48}$
Rainshowers	$Z = 370R^{1.31}$
Rain	$Z = 311R^{1.43}$

These relationships are the regressions of R as a function of Z as determined by Jones[2] from drop-size distributions taken in Illinois.

These rainfall rates were then combined with the 30-minute average areas for each step to give a mean network 30-minute rainfall amount for each 30-minute period, as indicated by radar. The radar 30-minute amounts are plotted against the gage 30-minute amounts in figure 1. The plot is on a logarithmic scale, and points which had either amount less than 0.0001 inch have not been plotted.

The scatter of points on the figure is quite large. A linear statistical analysis of these data yields a correlation coefficient of only 0.37 and a standard error of estimate of 0.048. This standard error of estimate is large in comparison with the mean 30-minute amounts of 0.041 and 0.033 inches for radar and gage, respectively.

Total storm amounts were found by summing all the 30-minute amounts. These are presented in table 1 and plotted in figure 2. The totals for 12 storms show the radar amount to be 26 percent higher than the gage amount. This discrepancy is not larger than might be expected at this range; however, it is surprising that the radar measurement is the higher one, since considerable attenuation was present in most of the storms. The storms of 4/20 and 5/23 had very strong attenuation. On 5/11 and 9/19, the rain was widespread, but of generally light rates. Widely-scattered small rain cells occurred on 6/8, 6/26, and 8/14; these had only brief periods of attenuation, if any at all. All other storms had varying degrees of attenuation during an appreciable portion of the rain.

TABLE 1

TOTAL STORM RAIN AMOUNTS FOR THE
KANKAKEE NETWORK, 1966

Storm Date	Total time in analysis (hrs)	Gage amount (in)	Radar amount (in)	Radar/gage ratio
4/20	1.5	.27	.0053	.020
5/11	12	.96	.81	.84
5/23	3	.88	.74	.84
6/8	3	.019	.14	7.4
6/8-9	6	.55	1.55	2.8
6/26	3.5	.089	.090	1.0
8/8	1	.034	.0091	.27
8/10	7.5	.61	.27	.44
8/14	6	.11	.11	1.0
8/21	2	.13	.61	4.7
9/14	8.5	.43	.61	1.4
9/19	7.5	.015	.23	15.3
Totals	61.5	4.10	5.17	1.26

The extreme cases were those of 4/20 and 9/19. On 4/20, the gage amount was 51 times the radar amount. This was a case of a line of thundershowers oriented in a north-northeast to south-southwest direction. At the time the rain was falling on the network, there were thundershowers on almost the entire path from the radar to the network. This produced the severe attenuation indicated by the difference in the measurements of rain.

On 9/19, the radar indicated a mean network amount 15 times that shown by the gages. This was true in spite of considerable light to moderate rain over the path to the network. Investigation revealed that the freezing level was at approximately 10,000 feet on that day. Through most of the summer, it had been at 13,000 to 14,000 feet. Under normal refractivity conditions, the top of the 1-degree beam would be at approximately 9800 feet, only 200 feet below the freezing level. Therefore, it would be reasonable to assume that the "bright band" would have contributed to the enhancement of the reflectivity measurement, giving an exaggerated radar measurement of rain. This effect will generally be an important deterrent to the radar measurement of rain at long ranges during the colder seasons of the year.

The case of 6/8-9 presented an even more puzzling problem. Approximately 0.11 inch of the radar indicated rain occurred during the 1-1/2-hour period prior to any indication of rain by the gages. Records were examined carefully for timing errors, but none were found. The storm of 6/8 (1315-1615C) had a similar 1-1/2-hour period in the middle of the storm when radar indicated 0.02 inch of rain while the gages measured nothing. It would appear that in these cases, rain-sized drops were present aloft, but were not falling to the ground in sufficient quantities or in the right locations to be recorded on the gages. Some of this is probably due to updrafts; however, these 1-1/2-hour periods are somewhat long to be completely explained in this way.

Area-depth Analysis

Another type of analysis was performed using these data. This was an application of the area-depth techniques commonly used in hydrologic studies. It is based on the assumption that similar area-depth curves can be produced using either gage or radar data, if the gage and radar data are well related. It was anticipated that the radar could be calibrated against the network 30-minute amounts by comparing the area-depth curves.

Using the 30-minute amounts for each gage, cumulative distributions were plotted in which the ordinate is the percent of the network having a 30-minute amount equal to or greater than the amount indicated on the abscissa. Each gage was assumed to represent 1/16 or 6.25 percent of the network. Similar mean curves for storm total rainfall were made. One of these is shown in figure 3. These curves were then entered with the percent of the network area having echoes of a given gain step. The 30-minute amount corresponding to each step is then the 30-minute amount produced by a rainfall rate which is just barely discernible on that step.

The analysis technique has certain limitations. The principal difficulty was that in many cases, the echo areas corresponding to the higher gain steps (the less sensitive ones) were less than the 6.25 percent

of the network represented by a single gage. Although these areas are small, they represent high rainfall rates, and therefore contribute a significant amount to the mean network rainfall. Because of these difficulties, most of the effort was shifted to analyses described in the earlier sections of this report.

In table 2, the minimum discernible rainfall rates are tabulated for each step as determined by this area-depth method and as determined by the radar equation, calibration of the radar, and the appropriate Z-R relationships. Ten storms are tabulated; two of the storms were eliminated because of the extremely poor correlation of radar and gage rates. The means for the 10 storms are also shown.

TABLE 2

MINIMUM DISCERNIBLE RATES AS DETERMINED BY DIFFERENT ANALYSIS TECHNIQUES (in/hr)

	Step 1		Step 2		Step 3		Step 4		Step 5	
Storm	Area-Depth	Radar Equ.	Area-Depth	Radar Equ.	Area-Depth	Radar Equ.	Area-Depth	Radar Equ.	Area-Depth	Radar Equ.
5/11	.118	.064	.149	.124	.211	.319	.380	.839		
5/23	.372	.055	.566	.139	.790	.661	1.010	1.228		
6/8	.030	.085	.072	.171						
6/8-9	.142	.070	.246	.129	.356	.614	.482	1.563		
6/26	.108	.037	.284	.051						
8/8	.030	.015	.204	.021						
8/10	.042	.013	.126	.053						
8/14	.080	.021	.300	.089						
8/21	.017	.025	.041	.072	.092	.182	.155	.637	.254	1.176
9/14	.016	.007	.036	.043	.066	.086	.176	.122		
Means	.096	.039	.202	.089	.303	.372	.441	.878	.254	1.176

It can be seen from table 2 that for the lower-numbered steps (high sensitivity), the area-depth method gives a higher rate than the radar calibration method. This changes as the radar sensitivity decreases, so that steps 3, 4, and 5 show lower rates for the area-depth method.

Attenuation effects tend to reduce the area visible by the radar at any one step level. Thus, if the area-depth relationship is used to predict the radar rate, the radar rate will be higher when attenuation is present. This effect is easily noted on steps 1 and 2, where the

area-depth values tend to be 2 to 2.5 times as high as the rates determined in the traditional manner. If, indeed, this can be attributed solely to attenuation, which seems likely, an average attenuation of about 4 to 5 db was experienced in the range to the network. In principle, this amount might be added to the first 2 steps to provide some adjustment for the attenuation. However, at the less sensitive regions a comparable correction would seem to be inappropriate.

A second effect is more dominant at the higher rates. When the area within a particular isohyet is less than the size which is represented by one raingage, the area-depth relationship as determined from the raingages becomes poor. The probability of detecting the high cores by a point measurement decreases as the size of the core decreases. The radar, on the other hand, always measures these high core areas well.

Thus, when the radar area is used to enter an area-depth relationship, the rainfall rate predicted will frequently be too small. These effects can be noted in table 2. On steps 4 and 5, the area-depth relationships tend to be from 20 to 50 percent of the traditional rates. A part of this difference is the gage spacing error, and a part may be due to improper radar-rainfall relationships. There must be some effect of attenuation in these measurements for higher rates, as well. It may be noted that these higher rates are contributing a larger portion to the total rainfall amount than the higher rates from the raingages, and thus the radar estimates are tending to be higher than the raingage amounts. Since there is a multiplicity of possible errors in these higher rates, it is not considered as appropriate to correct these in the same manner as that suggested for the lower rates. Nonetheless, it will be considered, and the amounts calculated using some correction at all rates based on these average area-depth relationships.

This study does indicate that for 30-minute amounts, the cores of rainfall are not well measured by the raingage density of one gage per 25 square miles. Since the scatter of rates, as determined from the area-depth method, is as great as it is, the method fails to provide as reliable a calibration scheme for the radar as had been hoped. Nonetheless, this scheme for providing a radar calibration appears to be more promising than to calibrate with a number of point measurements over the raingages.

RADAR MAINTENANCE

CPS-9

Extensive overhaul and modifications to the CPS-9 radar were initiated. Some have been completed and others will be completed shortly. Massachusetts Institute of Technology gave the University of Illinois a

portion of their AN/CPS-9 XE3. The antenna from their radar was completely dismantled, inspected, and reassembled during the winter. All worn bearings and all grease seals were replaced with new parts. The antenna was then mounted on the tower in place of the AN/CPS-9 XE2 antenna. The replacement antenna has the original antenna drive units, so, for the first time a complete antenna system will be available. The major advantage of the new system will be much better elevation control. The hybrid system which had been in use was designed for an SCR 545 radar and was less than satisfactory. In addition, it is expected that since a complete mechanical rebuilding job was performed, the unit should at least be more reliable mechanically. Changes were also required in the automatic programming chassis to properly control the new drive system. During the changes to the drive control systems, changes in the gain stepping section were also made. These changes permit more flexibility in the operational sequences and have been designed so that some means of automatic data processing equipment might be easily added.

New cables have been installed between the antenna and modulator, as the old cables had deteriorated in the 12 years since they were, originally installed. During the rewiring, the main power to the CPS-9 was modified to better balance the electrical load between phases, which should improve the regulation and prevent frequent main fuse failures.

These changes and modifications are nearing completion, and the radar should be operational within the next few weeks.

TPS-10

The TPS-10 radar has also undergone extensive repairs during the winter. A continual problem with the TPS-10 had been the azimuth drive and azimuth data presentation. Formerly the drive system has been accomplished using an amplidyne and servo motor. The original TPS-10 did not have a motorized drive system and this system was adapted from another radar. Control of the amplidyne was from a gyro-stabilized differential synchro. This drive had become mechanically loose and did not respond well to control signals. In addition, the lags between control and antenna position signals varied with antenna speed and direction, making the synchro signals unuseable for azimuth data display. Since, in the manner in which the TPS-10 is operated, the ability to stop and position the antenna is not necessary, the entire drive and control system has been removed and replaced with a synchronous motor. The azimuth data recording system will be improved by the removal of the azimuth drive system, and also by the inclusion of a four digit encoder. Azimuth position will then be read and photographed directly in digital form.

FLAGSTAFF DROP-SIZE SPECTRA

Raindrop size spectra were determined at Flagstaff, Arizona during July-August 1966 through support under contract DA 28-043 AMC 02376. These data have proven very interesting and valuable to this contract. Strikingly different rainfall-rate-radar reflectivity relationships were found. The earlier data sampling on a world-wide basis was directed to the primarily wet climates, and of course these climates are of more importance in an Army operational sense than the more arid climates. Thus, the Flagstaff data gives an indication of the type of relationships that might be obtained in the arid regions with a monsoon and will permit better estimations of radar rainfall relationships for the climatic atlas which will be prepared under this contract. Although the majority of the analysis which follows was performed under AMC 02376, it is presented herein in order to document the new data in this series of reports on drop size distributions.

Radar-Reflectivity Relationships for Flagstaff

Table 3 shows the regression coefficients between rainfall rate and radar reflectivity. The calculations have been performed considering the radar reflectivity as the independent variable. In addition to the regression for individual days, there are grouped data for the high concentration days and for the low concentration days. The average for all cases is also shown. The coefficient, A, for these regressions is much higher than is usual. This is especially true for the days in August and in the low concentration group. For all of these data, it is apparent that there is a paucity of small drops. When the coefficient of the regressions is high, it is an indication that the low rainfall rates have large raindrops which contribute strongly to the reflectivity. Only one other storm day at any of the 8 other locations sampled by a drop camera had a coefficient as high as the individual August storms or the low concentration group.

Overall, these relationships show that the raindrops in Flagstaff are relatively large. This general tendency has been noted by other investigators. Foote[3] in a recent article gave a relationship of $Z = 520\ R^{1.81}$ for the Tucson, Arizona area. His relationship has a high coefficient although not as high as the low concentration cases. The exponent is much larger than that of the Flagstaff data. This larger exponent indicates the larger importance of large drops at the higher rainfall rates. Hardy[4] reports a relationship of $Z = 460\ R^{1.41}$ for a case on 31 July 1961 at Flagstaff. Thus, it appears that all drop size investigations in this area tend to have large coefficients. The drop size spectra given by Hardy show more 0.5 mm drops than were measured using the drop camera, but, apparently, there was an insufficient number to influence the R-Z relationship. Hardy attributes the high coefficient primarily to evaporation, which may indeed be quite effective in this area. However, as is shown later, this does not explain the differences of the high and low concentration cases. Hardy's regression is determined with R as the independent variable in contrast to all other data which uses Z as the independent variable.

TABLE 3

RADAR REFLECTIVITY-RAINFALL RATE RELATIONSHIPS
FROM FLAGSTAFF

Date or Group	$Z = AR^b$ A	b	Correlation Coefficient	Standard Error of Estimate	No. of Cubic Meters in Sample
7/18	577	1.58	0.981	0.120	20
7/21	439	1.44	0.984	0.103	101
7/25	569	1.54	0.891	0.132	21
7/27	493	1.42	0.990	0.093	42
7/29	566	1.61	0.954	0.131	61
8/2	830	1.43	0.960	0.158	36
8/8	904	1.62	0.986	0.093	61
8/10	884	1.60	0.972	0.113	100
			* * * * *		
High Concentration	490	1.47	0.979	0.123	245
Low Concentration	889	1.55	0.974	0.128	197
All Data	593	1.61	0.969	0.153	442

The relationships from the Flagstaff data do not scatter about the regression line as much as the data from other locations. The standard error of estimate is a good measure of this scatter despite the failure of the data to be normally distributed. As can be noted from Table 3, the standard error of estimate varies from 0.09 to 0.158. Most of the values are near 0.13. This is contrasted to Miami data, where the standard error of estimate is around 0.17 on the average., with values of 0.2 not uncommon. From this it may be argued that there is a more consistent relationship in these data than elsewhere; a statement which seems to be supported by the lack of as much short time variability of rainfall rates as predicted from drop size data. Thus, it would seem that this supports the validity of the one-cubic-meter sample as being more nearly adequate in the Flagstaff rain than elsewhere.

The relationships predict a greater amount of radar return at Flagstaff for the same rainfall rate than the other locations for which drop size spectra are available. This seems somewhat paradoxical, since it has been observed that the non-precipitating clouds are less likely to be seen by radar in this area than central Illinois (Jones, et al.[5]).

As discussed elsewhere, the lack of scattering from the clouds may be due in part to extremely high concentrations of small cloud droplets although the concentration of raindrops at ground level appears to be abnormally low.

It may be noted that when the high and low concentration data are combined, the resulting relationship has a larger standard error of estimate. This is to be expected, of course. The exponent from this relationship is larger or equal to any of the individual exponents and is approaching the value from Foote's data. All of the regressions have been determined considering the reflectivity as the independent variable. If the rainfall rate had been considered as the independent variable, the coefficients would be higher and the exponents lower.

During preliminary data analysis, two different regimes of rainfall were noticed. Before speculating on the reasons for these differences, some of these differences will be examined.

Differences in Drop Concentration

The total number of raindrops per cubic meter of air space will be referred to as the concentration. Figure 4a-d shows concentration versus rainfall rate for 4 days. It should be noted that the two graphs on the left of the page have higher concentrations than the two on the All of the Flagstaff data tend to separate easily into these two groups which will be called the high and low concentration groups. The differences in concentration are sufficiently large to make it highly improbable that the differences are a result of sampling error or of any sorting effects of either the raindrop camera or of its immediate surroundings. There are a few points which overlap from one group to the other.

There were 5 days in which the concentrations were high. These dates were July 18, 21, 25, 27, and 29. There were three days, August 2, 8, and 10, in which there were low concentrations. If the high concentration cases are compared with data from other locales, it is found that the differences are not great. On an individual day basis, there were days at Miami which produced concentrations greater than the highest concentration but, after examining the data, there were no cases of concentrations as low as found on August 8 and 10.

It was conjectured that perhaps the raindrop camera in some way was faulty. One possible difficulty would have been that the focusing was incorrect so that the volume sampled was incorrectly judged. That is to say that, if the point of best focus were inside one of the shelters, the drops measured would have been only those in a small volume near the shield where the focus point was located. If this were true, the rainfall rates calculated from the drop camera would have been lower than actual. Table 4 has a comparison of the drop size data and the raingage data for these

4 days. The drop camera amount is obtained by integrating the calculated rainfall rates. Since the rates from the drop camera integrate to values of rainfall somewhat larger than determined by the raingage, the thesis that there is large instrumental error of this type is untenable and is rejected. For all cases but August 8, the drop camera was operated for 15 seconds of each one-minute period. On August 8, the camera was operated continuously during the minute. It may be fortuitous, but this may account for the better agreement on this day than others. In general, at other locations the drop camera amounts have tended to be less than raingage amounts by 10 to 15 percent. This has been attributed to either errors in the terminal velocities of the raindrops or to wind sorting effects of small drops in the vicinity of the raindrop camera shelters.

TABLE 4

COMPARISONS OF RAINFALL AMOUNTS FROM THE RAINGAGE AND FROM THE RAINDROP CAMERA

Date	Amount of Rain (mm) Raingage	Amount of Rain (mm) Drop Camera	Percentage Error + Indicates an Excess of Drop Camera	Duration of Rain (minutes)	Max Rate Drop Camera mm/hr
8/8/66	2.8	2.88	3	19	37.1
8/10/66	2.8	2.96	6	31	51.7
7/27/66	6.3	5.40	-14	44	49.3
7/21/66	8.6	9.20	7	92	76.6

The drop data were separated into the two groups of low and high concentration, and average distributions calculated for each group. These average distributions, shown in figures 5 and 6, are separated into rainfall rate intervals and serve to reduce the sampling noise considerably. The resultant distributions, particularly in the high concentration group, appear to be reasonably smooth spectra. From previous work, it has been noted that logarithmic normal distribution is the best fitting equation for drop size spectra. Values from the log normal fitting curve are plotted as x's on multiples of 0.5 mm. At the very least, the log normal curve provides an excellent means of further smoothing the data. Thus, values of the modal diameter, width of the spectra, rainfall rate, and liquid water content can be calculated from the log normal parameters. In most cases the results of computing the rainfall rate from the average distribution directly compare favorably with the calculation from log

normal coefficients. There are two notable exceptions. If the number of cubic meters in the average distribution is small and if there are a few large drops, there is a significant difference in the calculated rates. This is true because of the poor estimate of the average number of large drops due to small sample volume. This is the case in figure $6K_1$, where the distribution rate is 67.8 and the log normal rate is 87.28. In this case there are only 3 cubic meters of sample so that for any interval, a concentration less than $0.3/m^3$ cannot be measured. The other exception occurs with an obvious misfit of the log normal curve. Such cases are demonstrated by the lowest and highest rainfall rates of the low concentration case.

With these exceptions noted, the log normal parameters were used to calculate the diameter of the mode, B_m, the width of the spectrum at 1/2 number of the mode points, W, and the mean volume diameter, D_v. The mean volume diameter is defined as the size of drop whose volume multiplied by the concentration yields the liquid water content.

The three statistics, D_m, D_v, and W are plotted in figure 7 as a function of rainfall rate. The width remains nearly 0.5 mm larger for the low concentration case for all rates. In both cases the width increases with rainfall rate. It can be noted that these two groups of data do have much different characteristics.

There is a tendency for some of the curves to converge at the higher rainfall rates. This may indicate that whatever the mechanism which is producing these distinct groups, it may become less important at the higher rainfall rates. Unfortunately, this conclusion does not help much in eliminating possible reasons for these discrepancies since evaporation, cloud seeding, and drop generation mechanisms may all be less effective when the dynamics of the storm become the overwhelming force in producing rain.

As in previous data, the diameter of the mode of the distribution tends to pass through a maximum and decrease as the rainfall rate increases. In the low concentration case, this maximum is at 3 to 4 mm/hr. The high concentration case has its maximum at 10-15 mm/hr. Miami data has a peak of the mode at rainfall rates of 40-50 mm/hr. One explanation of these differences is the evaporation which takes place after the raindrops leave the cloud. Evaporation, which will be discussed in detail later in the report, tends to produce the effect of increasing the diameter of the mode. Further, it appears that at high rainfall rates evaporation becomes less important and the modes shift to lower values. Thus, if the low concentration is due to increased evaporation, it is reasonable to expect the maximum mode to occur at lower values of rainfall rate.

Differences in Spectra

There are a number of conditions which may have produced the differences in spectra. These are cloud modifications by silver iodide

seeding, evaporation, droplet growth by sublimation or coalescence, and a sampling error by virtue of either wind or gravitational sorting. These will be discussed in the ensuing paragraphs, but at the onset it should be pointed out that the ability to reach a firm conclusion on the basis of this rather limited sample is impossible. Some of the hypotheses would seem more likely than others, but none can be completely eliminated.

Silver Iodide Seeding

Meteorology Research, Incorporated, under contract from the Bureau of Reclamation, was conducting an experiment in weather modification in the Flagstaff area concurrently with this investigation. This group seeded with silver iodide generators from both ground stations and from aircraft. A personal communication from D. M. Takeuchi of MRI indicated, based upon a preliminary analysis, the days during which he felt that their seeding activities could have influenced the rainfall in the vicinity of the drop camera site. This information, along with the analysis of the raindrop spectra, is shown in table 5.

TABLE 5

COMPARISONS OF MRI SEEDING ACTIVITIES
WITH DROP SIZE SPECTRA

Date	Influenced by Seeding	Concentration Class	Notes
7/18	Yes	High	
7/21	Yes	High	
7/25	No	?	Small sample and rates < 1 mm/hr
7/27	Yes	High	
7/29	Yes	High	
8/2	No	Low	
8/8	Yes	Low	
8/10	No	Low	

On 7/25, Takeuchi did not believe that the seeding would have affected the drop camera spectra. Notes taken at the MRI debriefing would indicate that there was considerable doubt as to the location of the silver iodide. There were only 14 spectra obtained on this day and the rates were all very low, but if a decision as to which group had to be made, this day would have to be considered as a high

concentration day. The data on 8/8/66 are complete and there is no doubt that this is a low concentration day. There is some doubt as to whether the silver iodide was ingested by the rain cloud over the camera. Seeding was accomplished northwest of the San Francisco peaks with light and variable winds. The radar echoes on this day did move from the northwest, but at relatively low speeds.

The agreement between high concentrations and silver iodide seeding suggests that the silver iodide is affecting the rainfall mechanism. Furthermore, such an effect is in the direction which would be expected from the physics of cloud seeding.

The high concentration group contains spectra which are similar to spectra from other locations. The concentration-versus-rate relationship is about the same as was obtained at Miami, Florida. It may be argued that evaporation effects and ice nuclei deficiencies are more prevalent in Flagstaff than in Miami, and seeding is required to bring the storm system to equivalent states.

If it is assumed that the silver iodide seeding was the prime reason for the spectra differences, there remains the necessity of explaining why the unseeded spectra are so different from those obtained elsewhere. The data from Foote appear to be as closely related to the low concentration days as to the high., and thus, it cannot be categorically stated that the low concentration days are not the normal situation.

Gravitational and Wind Sorting Effects

It is conceivable that on the edges of shower cells, a drop size spectrum may exhibit unusually large drops and thus a lower concentration for a given rainfall rate. It is common to experience large drops at the onset of rain at a point, and if it is assumed that for the entire rain period an observer was located on the edge, a biased estimate may well result. In an attempt to evaluate the possible occurrence of this bias, the data from the MPS-34 radar were examined. A brief summary of the radar observations for 4 days of good camera data follows.

On 7/27 between 1210 and 1300, an echo formed just south of the drop camera. This echo intensified and moved slowly northward during the data collection. The echo developed an anvil which spread westward during the heavier rainfall periods. By 1240, the core of the storm had passed just east of the drop camera and was located northeast of the site. The rainfall gradient was very sharp. By 1245 there remained only light echo over the site with rainfall rates from the drop camera of 0.1 to 0.3 mm/hr. It would appear that all parts of this storm were sampled sufficiently.

On 8/8/66, two echoes passed over the drop camera. The first data at 1310 were taken when the core of the first echo was east of the site. The echo moved southeastward and changed from a large (7-mile diameter) echo into a number of smaller and less intense echoes. At 1320, a small cell was located west of the site. This second cell grew rapidly and passed directly over the drop camera. This second cell became more intense than the first echo, but did not grow to the same size. By 1340, the second cell was the only echo remaining, and had passed beyond the drop camera. On this day, the data may have been biased somewhat by the first cell, but the second cell tracked directly over the site. It was, however, in a growing stage during its passage and this may have contributed some bias.

On 7/21, the rain was from a very large echo which was centered southwest of the radar. This echo moved northward during the course of the observations. Within the large echo mass, several cells were included. The rain was quite general. It is not likely that any edge effect or growth phase was unduly biasing the drop camera results.

On 8/2/66 the rain began at the camera at 1403 falling from showers to the east of the site. The rain was to light at this time to be measured by the raingage with an over-sized receiver. By 1433 a developing cell southeast of the camera had moved and grown sufficiently to the northwest to have the camera near the center of the heaviest rain. The heaviest rain continued to fall over the camera until 1500 when the cell began to dissipate and move to the north. Thus, the camera photographed the raindrops from a shower which was over the camera during its maximum development and should not have an undue amount of edge or growth bias.

Unfortunately, no radar data are available for 8/10. The radar waveguide broke on 8/9, eliminating the possibility of observations on 8/10, the last day that data were taken. The results of the radar analysis are mostly negative in that no apparent biases due to locations of the echo or growth phases can be discerned.

Evaporation Effects

Evaporation effects on drop size distribution tend to be more effective on the small raindrops. Thus, qualitatively one might expect that if rain fell through a dry, warm layer, the large drops would become more important in the resulting distribution. As a result, one might expect lower concentrations. Since, indeed, the climate of Arizona is such that evaporation may be quite significant, and the shifts are in the direction observed, an investigation of evaporative effects was undertaken.

Radiosonde data provided by the U. S. Army meteorological team gives the environmental temperatures and humidities on the days for which drop size data are available. An abstract of this data is shown

in table 6. No radiosonde data is available for 8/10. The data on 7/18 is extrapolated from an early morning sounding. On other days, it was usual to find very small changes in the moisture between the early morning sounding and the late morning sounding. It also was common for the temperatures between 700 mb and the surface to become nearly adiabatic between soundings. Thus, to estimate the surface temperature, humidity, and lifting condensation level, the adiabatic lapse rate from 700 mb temperature was used. There were no soundings on 7/19, but on the early morning sounding of 7/20, a considerable amount of moisture had entered the Flagstaff area. The surface mixing ratio changed from less than 5 g/kg on 7/18 to more than 12 g/kg on 7/20. Thus, it may be that the sounding on 7/18 is not representative of the rain time. The case of 7/18 is belabored, since it does not appear to fit with the rest of the data if evaporation is the cause of the concentration effects noted.

TABLE 6

ENVIRONMENTAL CONDITIONS ON DAYS
OF DROP SIZE DATA

	Time	Ground		300 mb		Height
	LST	RH	Temp	RH	Temp	LCL (km MSL)
7/18	*	35	25	42	14	4.1
7/21	1055	55	22.1	74	11.0	3.3
7/25	1040	56	22	59	13.5	3.35
7/27	1030	50	24.3	56	14.2	3.57
7/29	1210	63	22	78	12.0	3.1
8/2	1030	45	26.2	38	13.0	3.72
8/8	1000	48	23.2	48	14	3.7

* Estimated from 0530 7/18 sounding.

If the 7/18 is ignored, the two classes of high and low concentration are separable into two identical groups with respect to the humidity. The low concentration cases occur with surface humidities of 45 and 48%, while the high concentrations occur from 50 to 63%. The 7/27 case where the surface humidity is 50% is a marginally high concentration as mentioned previously. The humidity differences are even more pronounced at the 700 mb level. Here, the low concentration cases are much drier. The differences in lifting condensation levels are also apparent in these tables.

In an attempt to make the evaporation arguments more quantitative, the evaporative effects on drop size distributions from the lifting

condensation levels to the ground have been examined. Kinzer and Gunn[6] experimentally derived tables of rate of evaporation. Their equation (29) is:

$$\frac{dM}{dt} = 4\pi aD\ (\rho_a - \rho_b)\ (1 + \frac{Fa}{s'})$$

where $\frac{dM}{dt}$ = mass rate of evaporation and the two factors

$$4\pi a(1 + \frac{Fa}{s'}) \quad \text{and} \quad D(\rho_a - \rho_b)$$

are empirically determined and listed in tabular form. For convenience, let the first factor be called A and the second B. Then:

$$\frac{dM}{dt} = AB$$

Since:

$$M = \frac{\pi}{6} D^3$$

where D = diameter of the drop in cm and p = density of water

$$\frac{dM}{dt} = \frac{\rho\pi D^2}{2} \frac{dD}{dt}$$

and

$$\frac{dD}{dt} = \frac{2}{\pi\rho D^2} \frac{dM}{dt}$$

If the drop is falling at its terminal velocity V, then

$$\frac{dD}{dt} = \frac{dD}{dZ} \frac{dZ}{dt} = V \frac{dD}{dZ}$$

where Z = the height coordinate.

Combining and writing in differential form:

$$dD = \frac{2AB}{\pi\rho D^2\ V}\ dZ$$

For convenience in interpolating values, the initial drop size distribution at the ground will be approximated by the logarithmic normal

distribution. Let N(D) dD represent the distribution at ground level, and N(ξ) dξ the distribution which after undergoing evaporation yields N(D) dD at ground level. Then:

$$D = \xi - \frac{2\ AB}{\pi\rho\xi^2 V}\ \Delta Z$$

Table 7 shows the magnitude of changes of the drop diameters for the environmental conditions on 7/29 and 8/2.

As the diameter of the drop changes, the terminal velocity of the drop changes. This leads to the so called "Traffic problem". This can be compensated for by considering the number of drops within a volume defined by unit area in the horizontal and height equal to the terminal velocity. As the evaporation process continues and provided the drops do not completely evaporate, the number of drops in a new volume defined by unit area and the new terminal velocity will be the same as before.

Thus

$$N(\xi)\ d\xi\ V\xi = N(D)dDV_D$$

and

$$N(\xi) = N(D)\ \frac{V_D}{V\xi}\ \frac{dD}{d\xi}$$

This latter equation was programmed for steps of 100 m from the surface

TABLE 7

EVAPORATION EFFECTS ON DROPS FOR
JULY 29 AND AUGUST 2

Diameter at Ground Level (mm)	Diameter at Lifting Condensation Level (mm) 7/29	8/2
.5	0.85	1.17
1.0	1.23	1.44
1.5	1.65	1.81
2.0	2.11	2.24
2.5	2.60	2.71
3.0	3.09	3.20
3.5	3.59	3.70

to the lifting condensation level. These calculations were performed for each of the average distributions for the low and high concentration conditions. The nature of the problem is such that no information on the number of small drops aloft can be determined since these evaporate before reaching the ground. However if one examines only the concentration of drops larger than 2.0 mm, it can be seen that the evaporation does not make the two distributions similar although they are closer than initially. Table 8 shows the values for three of the lower rates for both concentrations. It can be noted that even after evaporation the number of drops in larger sizes is not comparable. Only the lower rates are considered since the evaporation is proportionally less for the higher rates. The rainfall rate calculated at the lifting condensation level (LCL) must be considered fictitious since the concentration of small drops is unknown. Thus this rate is only the rate from the larger drops which survive the fall to the ground. It may be noticed that the percentage increase in rainfall rates for the low concentration is always less than or equal to the percentage increase in the high concentration. That is to say the effect of the drier environment on the low concentration case is not sufficient to override the relatively large number of big drops.

TABLE 8

EVAPORATION EFFECTS ON CONCENTRATION OF RAINDROPS

Rainfall Rate at Surface mm/hr	Rate Aloft	Concentration Type L = low H = high	Number of Drops Between 2.0 and 2.5	Number of Drops Between 2.5 and 3	Number of Drops Greater than 3.0 mm
1.06	1.41	L	2.91	1.41	.75
.93	1.23	H	2.64	.35	.03
3.05	3.47	L	4.70	4.21	2.76
2.84	3.62	H	9.76	2.18	.46
4.94	5.72	L	8.23	6.31	4.39
3.98	4.93	H	13.69	4.08	1.07

Figure 8 shows 2 examples of the drop size spectra after evaporation has taken place. Again it would certainly seem that these two distributions are sufficiently different that evaporation cannot explain the differences noted between the high and low concentration cases.

In summary, evaporation apparently does explain qualitatively the high coefficient in the radar reflectivity rainfall rate relationship but does not explain quantitatively the differences between the different cases at Flagstaff.

NEW JERSEY AND NORTH CAROLINA DROP-SIZE DISTRIBUTIONS

Island Beach, New Jersey and Coweeta, North Carolina, two locations where raindrop-size data were collected with the raindrop camera, have been examined with regard to the raindrop-size distributions that exist in these areas. Island Beach, New Jersey, located on the Atlantic coast, has a humid continental climate modified to some degree by the ocean, while Coweeta, North Carolina, located in the southwestern portion of the state approximately 225 miles from the ocean, also has a humid continental climate. The actual location of the raindrop camera at Coweeta was at an elevation of 4450' MSL in the Nantahala Mountains, approximately 3/4 mile southeast of a mountain peak which is 5000' MSL in elevation, so orographic effects played a role when a southeasterly wind blew over the area. It is hoped that a knowledge of the types of drop-size distributions that exist in these regions will lead to accurate relationships between rainfall rate (R) and radar reflectivity factor (Z), which could ultimately result in a method whereby rainfall amounts for storms could be estimated remotely by radar. The one fact that greatly limits the accuracy of the radar to determine rainfall amounts is the apparent lack of consistency of the drop-size distributions for various meteorological conditions, and since radar reflectivity is directly dependent on drop-size diameter, one must know what the distributions look like. Even when these conditions appear to be nearly the same, the drop-size distributions do not remain constant. The approach that one takes is to stratify the data in such a way so as to include only those distributions that are the same or nearly so. Stratifying the data according to rain type, synoptic type, or degrees of stability associated with the precipitation have been found to be appropriate, with the latter two being the most effective in separating the data into nearly constant drop-size distributions.

Analysis of the Drop Spectra

In order to discover general trends and characteristics associated with the distributions, it was necessary to examine average drop-size spectra at each location, rather than individual minutes of data. The averages were determined as follows. The data from each of the two locations were sorted in ascending order according to rainfall rate, and then grouped into intervals 1.0 mm/hr wide at the lowest rates, increasing in size at higher rates. The average number of drops per cubic meter in each 0.1 mm increment of drop diameter from 0.5-7.0 mm, along with other related parameters, was calculated by a computer. For this part of the analysis all of the data were grouped together without stratification.

Upon examining the distributions from both areas, it was found that they are quite similar. Figures 9, 10a, 10b, and 10c reveal this

similarity. Figure 9 is a plot of N_T vs N_T, on log-log coordinates, where N_T is the total number of drops per cubic meter for a particular rain rate. The ordinate represents Coweeta, North Carolina and the abscissa represents Island Beach, New Jersey. Each point then represents the average total number of drops for each location for the same average rain rate. For low N_T'S, Coweeta has more drops for the same average rain rate while for the high N_T's, Island Beach has more drops; in the intermediate N_T range, both locations have approximately the same number of drops for the same average rain rate.

One may also examine rainfall rate (R) with regard to its relationship to certain diameters of the drop-size distributions namely, D_G, D_1 and D_M. D_G is the geometric mean diameter of the spectra with

$$\ln D_G = \frac{\sum_{i=1}^{i=n} n_i \ln D_i}{N_T} \qquad (1)$$

as described in an equation for a log normal distribution fit for the drop-size spectra; D_L is the median volume diameter which is the diameter of the drop-size where half of the liquid water content of the distribution, for the one cubic meter sample, lies above that drop-size and half below; D_M is the diameter of the size drop that occurs in the largest numbers. Figures 10a, 10b, and 10c show some representative drop-size distributions for the low, middle and high portions respectively of the N_T-N_T curve. Ng is the number of one minute samples used for each rate. Figures 11A, B, and C are plots of R vs D_G, D_M and D_L respectively, on log-log coordinates, revealing again the similarity of the spectra at both locations; the R vs D_L curves for both areas are nearly coincident. R vs D_G and D_M (Figs. 11A and 11B) also reveal a marked similarity for the two areas.

Rainfall Rate-Radar Reflectivity Relationships

The radar reflectivity factor (Z) from a single raindrop has been found to depend directly on the sixth power of the drop diameter (D), so the total reflectivity factor from any rain echo will be,

$$Z = \sum_{D=0.5}^{D=7.9} n_0 D^6 \qquad (2)$$

where n_D is the number of drops of diameter D. The spread of D from 0.5-7.9 mm best describes the drop interval that was encountered in the data collection; very few raindrops were found to be outside these values. Now, if one plots, on log-log coordinates, the R-Z values for each minute of data, the resulting curve would be a straight line, with no scatter of points around the line, if all the rains had the same distribution of drops where only N_T changes, and the relative percentage of each size drop remains the same for different rates. (There are other situations that would also result in a regression line with no scatter). Unfortunately, this is not true, so the result is a regression line with a great deal of scatter of points around the line. Unless this scatter is reduced appreciably, a rainfall rate or total rainfall amount evaluation from a known reflectivity would be subject to greater errors than could be tolerated for most purposes. It is desirable then to seek some means of stratifying the data in such a manner so as to result in a more meaningful R-Z relationship. Several parameters have been tried, but the ones found most effective have been synoptic type (cold frontal, warm frontal, etc), and PASI type (Positive Area Stability Index) of the rains, the PASI data being obtained from a thermodynamic diagram. For both locations, Island Beach and Coweeta, synoptic stratification was found to be slightly more effective than PASI. Tables 9-12 illustrate this point. Table 9, for North Carolina, lists the PASI intervals in joules per kg net area and the associated standard errors of estimate (S.E.E.) for each PASI interval; Table 10 lists the synoptic stratifications and their associated S.E.E. Tables 11 and 12 contain similar information for New Jersey. When the S.E.E. for the synoptic separation is greater than that for all the data combined, one should use the latter R-Z relationship.

The regression lines, when synoptic stratification was employed, reveal some interesting observations regarding the drop-size distributions in warm frontal and cold frontal rains. First, it should be noted that within each of the above frontal patterns, there are variations; for example, there are slow and fast moving cold fronts resulting in stratiform type clouds in the former and cumuloform clouds in the latter. So, when a statement is made concerning the drop spectra in warm and cold frontal situations, it must be realized that the meteorological conditions such as wind shear, convection, evaporation etc. associated with the fronts do not necessarily remain constant. However, if several cases of frontal rains are examined, one expects to find that the drop-size distributions in warm frontal rains would tend to be composed of smaller drops than for similar rainfall rates in rains associated with cold fronts. Warm front precipitation is generally of the steady variety, with fog and drizzle often occurring simultaneously with the rain resulting in smaller overall drop-sizes. Cold front rains tend to be associated with convective clouds resulting in showery type precipitation and larger drops than found in warm front rains of similar rates. Since radar reflectivity is directly related to the drop-sizes (2), it follows that cold front rains in general, should have higher reflectivities than those of warm fronts for similar rainfall rates. Atlas and Chmela[7] found this to be the case

TABLE 9

REGRESSION PARAMETERS FOR
NORTH CAROLINA PASI STRATIFICATION

PASI Interval joules/kg	A (regression coefficient)	b (regression exponent)	N_s (No. of samples in regression)	S.E.E. (Standard error of estimate)
-120,000 to -140,000	280	1.32	417	.161
-100,000 to -120,000	259	1.38	948	.163
-75,000 to -100,000	225	1.38	590	.168
-50,000 to -75,000	206	1.55	283	.180
-50 to -700	243	1.35	652	.176
-0 to -50	215	1.45	327	.167
0 to 50	196	1.47	227	.151
50 to 500	213	1.35	467	.176
500 to 1,000	234	1.36	112	.142
1,000 to 4,500	241	1.34	440	.138
All Data (No Stratification)	234	1.39	4721	.170

TABLE 10

REGRESSION PARAMETERS FOR
NORTH CAROLINA SYNOPTIC STRATIFICATION

Synoptic Class	A (regression coefficient)	b (regression exponent)	N_s (No. of samples in regression)	S.E.E. (Standard error of estimate
Airmass	248	1.38	915	.167
Airmass Orographic	217	1.30	87	.145
Pre-cold Frontal	218	1.38	284	.161
Pre-cold Frontal Orographic	164	1.58	31	.241
Cold Frontal	208	1.39	346	.156
Cold Frontal Orographic	183	1.48	204	.195
Post Cold Frontal	238	1.35	594	.161
Overrunning	253	1.43	880	.167
Overrunning Orographic	197	1.33	59	.137
Warm Frontal	220	1.39	662	.169
Warm Sector	279	1.36	138	.093
Cold Occlusion Concurrent	157	1.34	100	.175
Pre-cold Occlusion	277	1.62	252	.147
Pre-cold Occlusion Orographic	311	1.67	71	.119
Post Cold Occlusion	223	1.26	62	.128
Trough Aloft	188	1.39	36	.233

TABLE 11

REGRESSION PARAMETERS FOR
NEW JERSEY PASI STRATIFICATION

PASI Interval joules/kg	A (regression coefficient)	b (regression exponent)	N_s (No. of samples in regression)	S.E.E. (Standard error of estimate)
-130,000 to -160,000	252	1.37	627	.148
-100,000 to -130,000	241	1.45	601	.143
-80,000 to -100,000	318	1.57	395	.174
-50,000 to -80,000	241	1.37	199	.139
-0 to -500	255	1.32	232	.198
0 to 50	268	1.56	301	.141
50 to 500	226	1.27	203	.155
500 to 1,000	258	1.45	228	.133
1,000 to 2,500	230	1.31	103	.228
All Data (No Stratification)	256	1.41	3124	.163

TABLE 12

REGRESSION PARAMETERS FOR
NEW JERSEY SYNOPTIC STRATIFICATION

Synoptic Classification	A (regression coefficient)	b (regression exponent)	N_s (No. of samples in regression)	S.E.E. (Standard error of estimate)
Airmass	293	1.39	325	.143
Pre-cold Frontal	322	1.56	87	.138
Cold Frontal	207	1.32	362	.162
Post Cold Frontal	221	1.43	347	.141
Overrunning	265	1.37	413	.129
Warm Frontal	268	1.47	749	.179
Cold Occlusion Concurrent	349	1.62	73	.173
Tropical Storm N. W. Sector	205	1.30	33	.236
Trough Aloft	260	1.37	14	.105
Northeaster	271	1.40	654	.142

indicating that heavy showers and large coefficients (in the Z-R equation) showed a preference for occurring with cold fronts. The coefficient refers to that parameter of the regression line which determines the Z intercept of the line; the general equation for the regression line is

$$\text{Log } Z = \text{Log } A + b \text{ Log } R \qquad (3)$$

where A is the coefficient of R when antilogs are taken in (3). The slope of the regression line given by (3) is represented by "b".

The values for A and b, for the warm and cold fronts, as well as the number of samples available from each location, are listed in Table 13. Related information for Miami, another area where raindrop data were collected, is also presented. It is immediately obvious from an examination of these data that the warm frontal rains for all three locations, have larger coefficients than the cold frontal rains which is certainly an unexpected result. Figure 12 shows some comparisons of drop-size spectra for warm and cold front rains from Island Beach and Coweeta, for representative spectra of similar rainfall rates. In each case, the warm frontal rain shows a greater number of the larger size drops, (from 1.5 mm diameter upwards, in 3 out of the 4 cases). With the number of samples from each area being relatively large and the data being obtained from several storms in each area, the results are quite surprising. These data definitely indicate that cold front rains, at least in the areas where the data were obtained, generally consist of smaller drops than warm front rains of similar rates.

TABLE 13

COLD AND WARM FRONT REGRESSION PARAMETERS

	A (regression coefficient)	b (regression exponent)	N_s (No. of samples in regression)
North Carolina:			
Cold Front	208	1.39	346
Warm Front	220	1.39	662
New Jersey:			
Cold Front	207	1.32	362
Warm Front	268	1.47	749
Miami:			
Cold Front	198	1.54	187
Warm Front	403	1.24	341

At this point, an examination of the variables effecting drop-size distributions would be desirable in an attempt to explain the apparent contradiction. Assuming some given initial drop-size distribution, the following factors may effect the distribution: accretion, evaporation and wind shear sorting. Qualitatively, wind shear sorting and evaporation would tend to produce changes in the initial distribution resulting in larger coefficients in the regression equation. This would mean larger drops for similar rainfall rates. Accretion of cloud droplets, on the other hand, would tend to have a decreasing effect on the regression coefficient of the original distribution resulting from a larger importance of the smaller drops (Atlas and Chmela[7]). Also, in initial warm frontal precipitation, where all of the rain originates in the warm air above the front, evaporation is high as the drops fall into the cooler, dryer air below the front, resulting in spectra weighted towards relatively large drops. As the front becomes more developed, the evaporating rain forms clouds below the front, increasing the moisture content, and evaporation of the subsequent falling drops is considerably reduced. Along with this, drizzle and fog often exist in well developed warm frontal situations where small drops are superimposed onto the precipitation formed in the frontal zone aloft. As a result, the overall effect in well-developed warm fronts on drop-size spectra is an increase in the number of small drops reaching the ground. One may postulate then, assuming that accretion, evaporation and wind sorting all occur in varying degrees, and that nature begins with the same drop-size distribution in the clouds, that evaporation and wind sorting are more pronounced in warm frontal rains than those associated with cold fronts, in the areas where the raindrop data were taken. Indirectly, this is also saying that warm fronts in these areas generally are not associated with low level clouds and drizzle, or that cold fronts are characterized by little raindrop evaporation and a great deal of accretion of cloud droplets during rain formation when compared to warm fronts. The latter appears to be a more plausible explanation at this time. Lamp[8] found that drop-size distributions in an active cold front rain of the convective cloud variety, were very much like those found in three warm front rains on which he had data; all were composed of relatively small drops.

Drop Spectra in Orographic Rains and Tropical Storms

The location of the raindrop camera at Coweeta, North Carolina, as was noted in the introduction, was quite favorable for orographic precipitation when a southeasterly wind blew over the area. Some 300 minutes of data involving orographic rains were obtained. It was quite fortunate that data were available from synoptic classifications of the same type with and without orographic effects; this allowed for a comparison between the two. The associated R-Z relationships are shown in Table 14. It may be seen that, in 4 out of 5 cases, the synoptic classification involving the orographic rains had smaller coefficients than the same classification without the orographic effects. This indicates that the drops are generally smaller for the orographic cases, for the same or similar rainfall rates. Work done by Weaver[9] agrees with this conclusion.

TABLE 14

REGRESSION PARAMETERS FOR
NORTH CAROLINA OROGRAPHIC RAINS

Synoptic Class	A (regression coefficient)	b (regression exponent)	N_s (No. of samples in regression)	S.E.E. (Standard error of estimate
Airmass Orographic	217	1.30	87	.145
Airmass	248	1.38	915	.167
Pre-cold Frontal Orographic	164	1.58	31	.241
Pre-cold Frontal	218	1.38	284	.161
Cold Frontal Orographic	183	1.48	204	.195
Cold Frontal	208	1.39	346	.156
Overrunning Orographic	197	1.33	59	.137
Overrunning	253	1.43	880	.167
Pre-cold Occlusion Orographic	311	1.67	71	.119
Pre-cold Occlusion	277	1.62	252	.147

On September 19, 1961, tropical storm Ester, the remnants of Hurricane Ester, passed well offshore from the raindrop camera at Island Beach, New Jersey, causing some light precipitation as its outer fringes brushed the coast. A very limited amount of data were recorded by the camera (33 minutes). However, it would be of interest to present the results, keeping this in mind. The R-Z equation for this case is:

$$Z = 205R^{1.30} \qquad (4)$$

The scatter around the regression line is noticeably more for this case when compared with the other stratifications. The S.E.E. is .236 as compared with .178 for the group with the highest S.E.E. of the remaining classifications; the small number of samples is partially responsible for this. It appears

that tropical storms may indeed contain small drops when compared to other synoptic types. A comparison of cold and warm front rains, and the tropical storm data is made for similar rainfall rates in Figure 13. It indicates that the tropical storm is composed of many small drops and few large ones when compared to the other distributions.

SUMMARY AND CONCLUSIONS

The results from the Kankakee Network radar-rainfall studies show greater errors in the measurements than would be desired. Further investigations of these data, and new data from 1967 operations, should provide a better understanding of these errors and provide ways of recognizing by radar those situations in which accurate measurements of rain at extended ranges are not possible.

The rainfall-reflectivity relationships from Flagstaff, Arizona are significantly different from those previously reported for other locations. The distributions of raindrop size fall into distinctive groups, one having a much higher concentration of drops than the others. Several possible causes for these differences were examined, none of which were found to be completely adequate.

The drop-size distributions from New Jersey and North Carolina are quite similar. It was found that the best means of stratifying the data for rainfall rate-radar reflectivity relationships is according to synoptic type for these areas. Cold front rains were found to *be* composed of smaller drops than warm front rains for similar rainfall rates. Orographic rains had smaller drops than rains of similar synoptic conditions without orographic effects. A small sampling of tropical storm rain in New Jersey had smaller drop-sizes than most other spectra.

REFERENCES

1. Probert-Jones, J. R., 1962. The radar equation in meteorology. Quart. J. R. Meteor. Soc., 88, pp. 485-495.

2. Jones, D. M. A., 1956. Rainfall drop size-distribution and radar reflectivity. Illinois State Water Survey, Research Report No. 6 under Contract DA-36-039 SC-64723, Signal Corps Engineering Laboratories, Fort Monmouth, N. J.

3. Foote, G. B., 1966. A Z-R relation for mountain thunderstorms. J. Appl. Meteor. 5, No. 2, pp. 229-231.

4. Hardy, K. R. , 1962. A study of raindrop-size distributions and their variation with height. Univ. of Michigan, Dept. of Engineering Mechanics, Scientific Report No. 1, Contract No. AF19(628)-281, p. 81.

5. Jones, D. M. A., R. E. Rinehart, E. A. Mueller, and D. W. Staggs, 1967. Evaluation of the maser-equipped radar set AN/MPS-34 and area precipitation measurement indicator. Illinois State Water Survey, Final Report on Contract No. AMC-02157(E), Atmospheric Sciences Laboratory, Fort Monmouth, N. J.

6. Kinzer, G. D., and R. Gunn, 1951. The evaporation, temperature and thermal relaxation time of freely falling water drops. J. Meteor., 8, No. 2, pp. 71-83.

7. Atlas, D. and A. C. Chmela, 1957. Physical-synoptic variations of raindrop size parameters. Proc. 6th Weather Radar Conf., Cambridge, Mass. pp. 21-29.

8. Lamp, R., 1958. Das Tropfenspektrum in Niederschlägen und die Radar-Reflectivität nach fremden und eigenen Messungen. Beiträge zur Physik der Atmosphäre, 30, pp. 223-245.

9. Weaver, R. L., 1966. California storms as viewed by Sacramento radar. Mon. Wea. Rev., 94, No. 7, pp. 466-474.

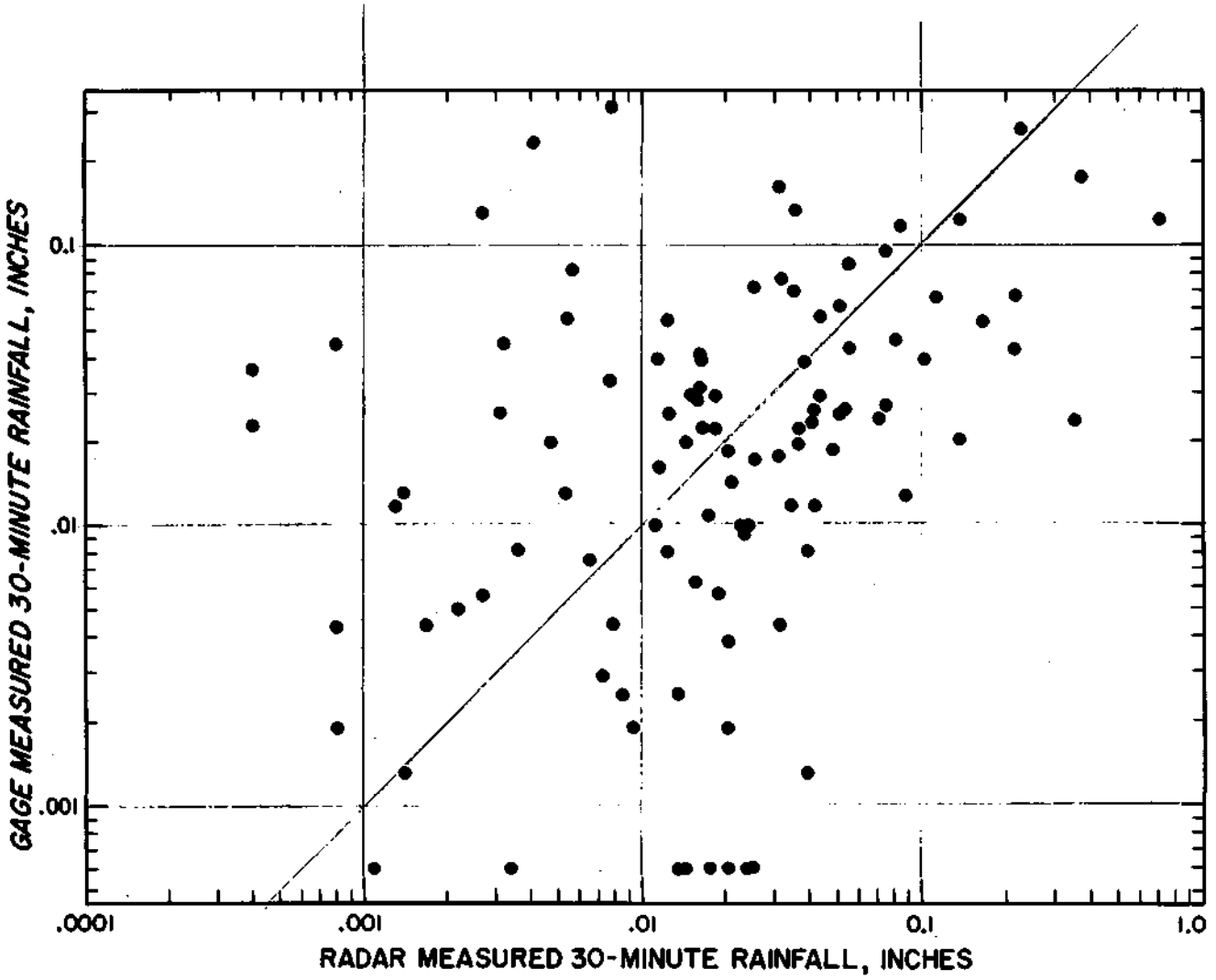

Fig. 1. Radar and gage measured 30-minute rainfall for the Kankakee Network.

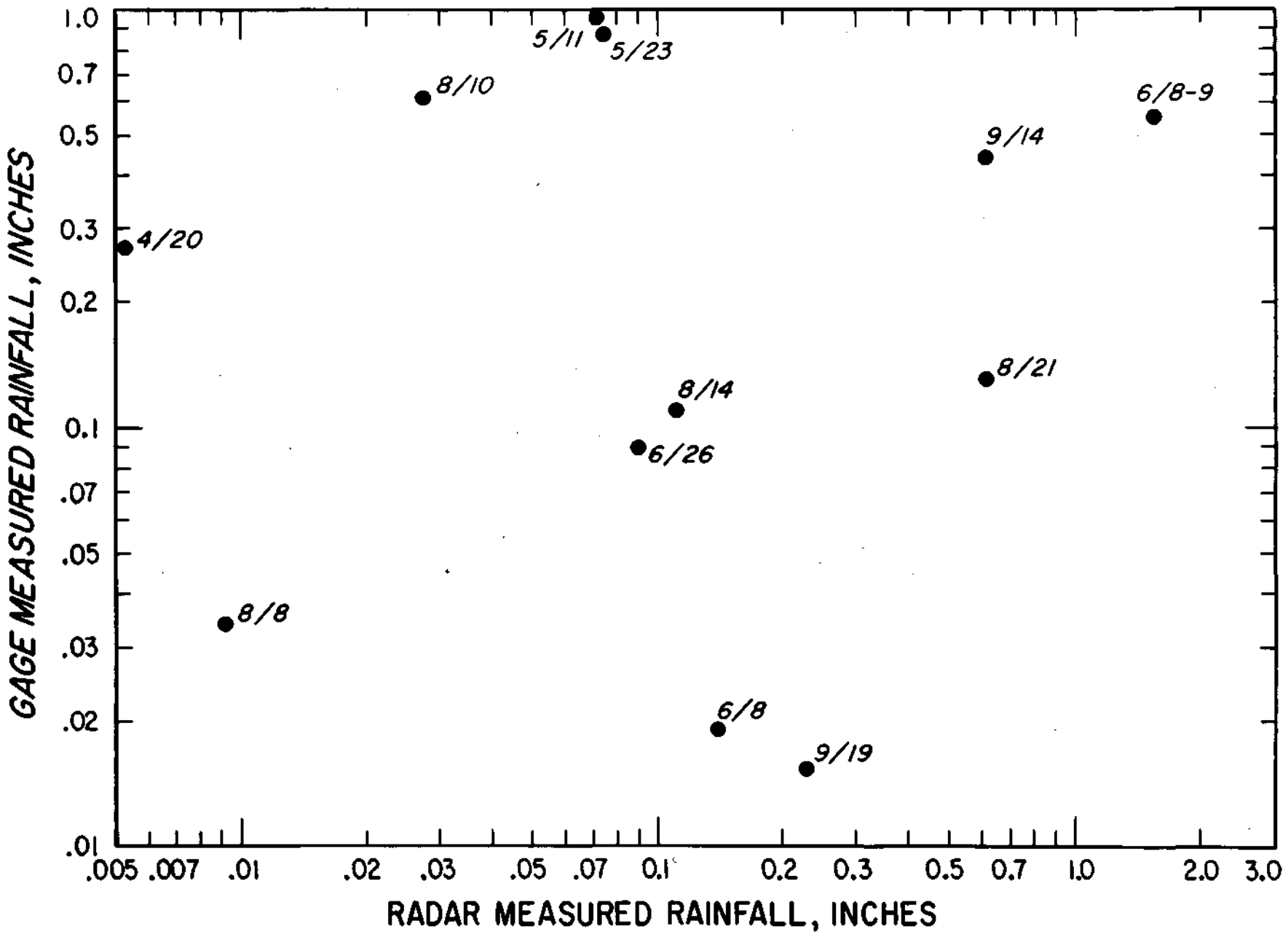

Fig. 2. Radar and gage measured total storm rainfall for the Kankakee Network.

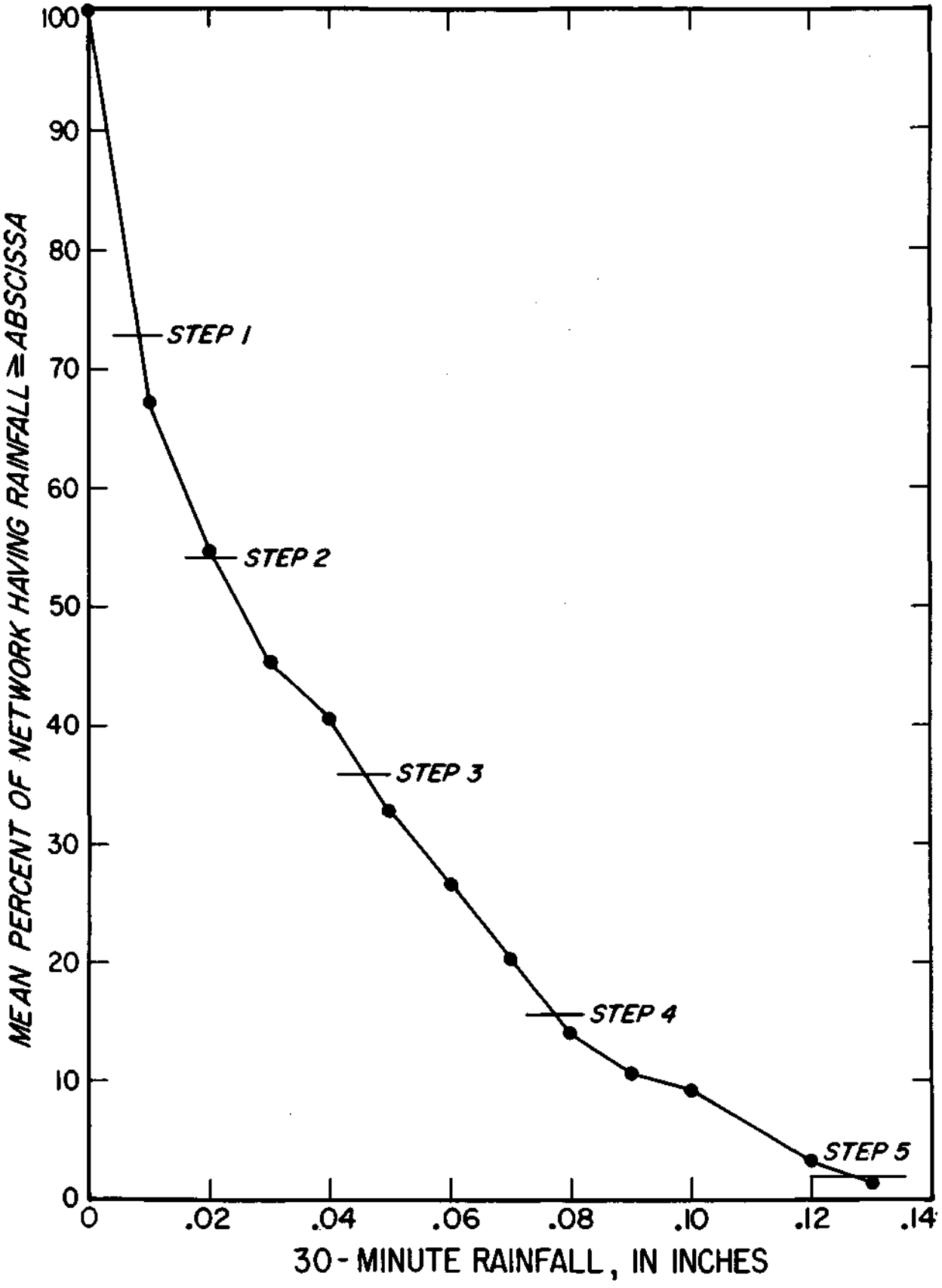

Fig. 3. The mean storm area-depth curve for the 8/21 storm on the Kankakee Network, showing the percent of the network covered by echoes on each gain step.

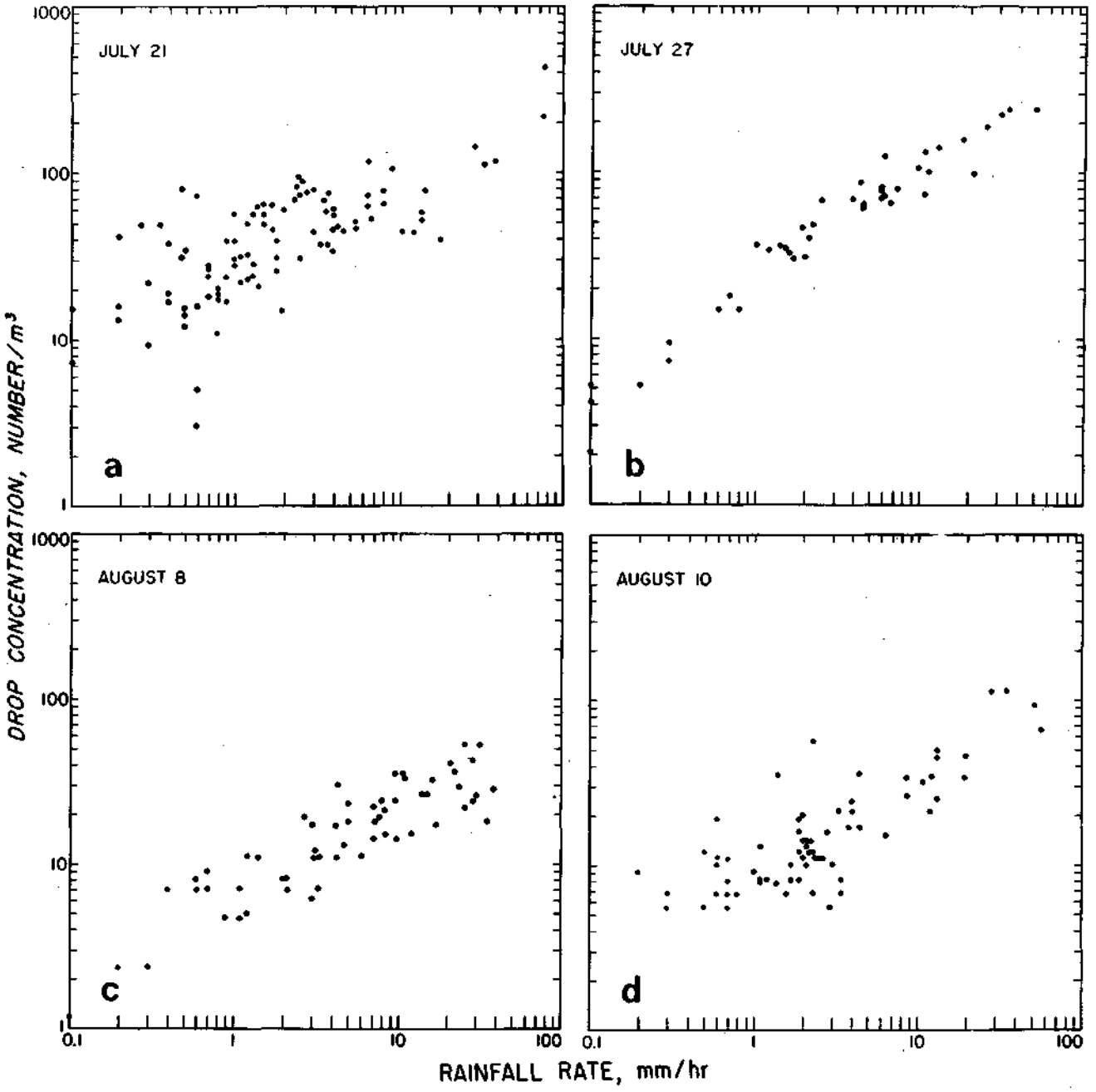

Fig. 4. Drop concentration vs. rainfall rate at Flagstaff, Arizona on the dates indicated.

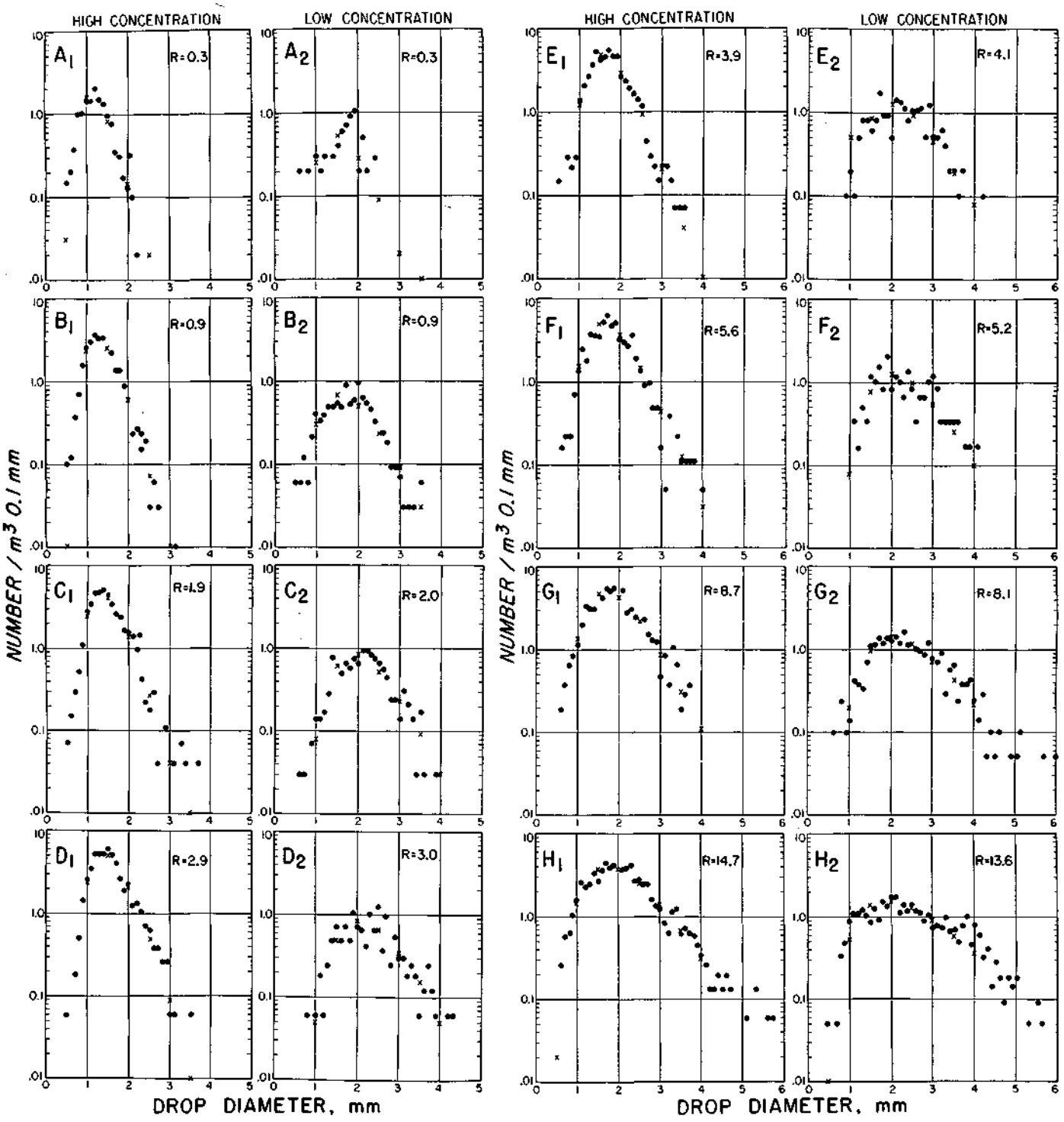

Fig. 5. Average drop-size distributions for the low and high concentration cases at Flagstaff, Arizona.

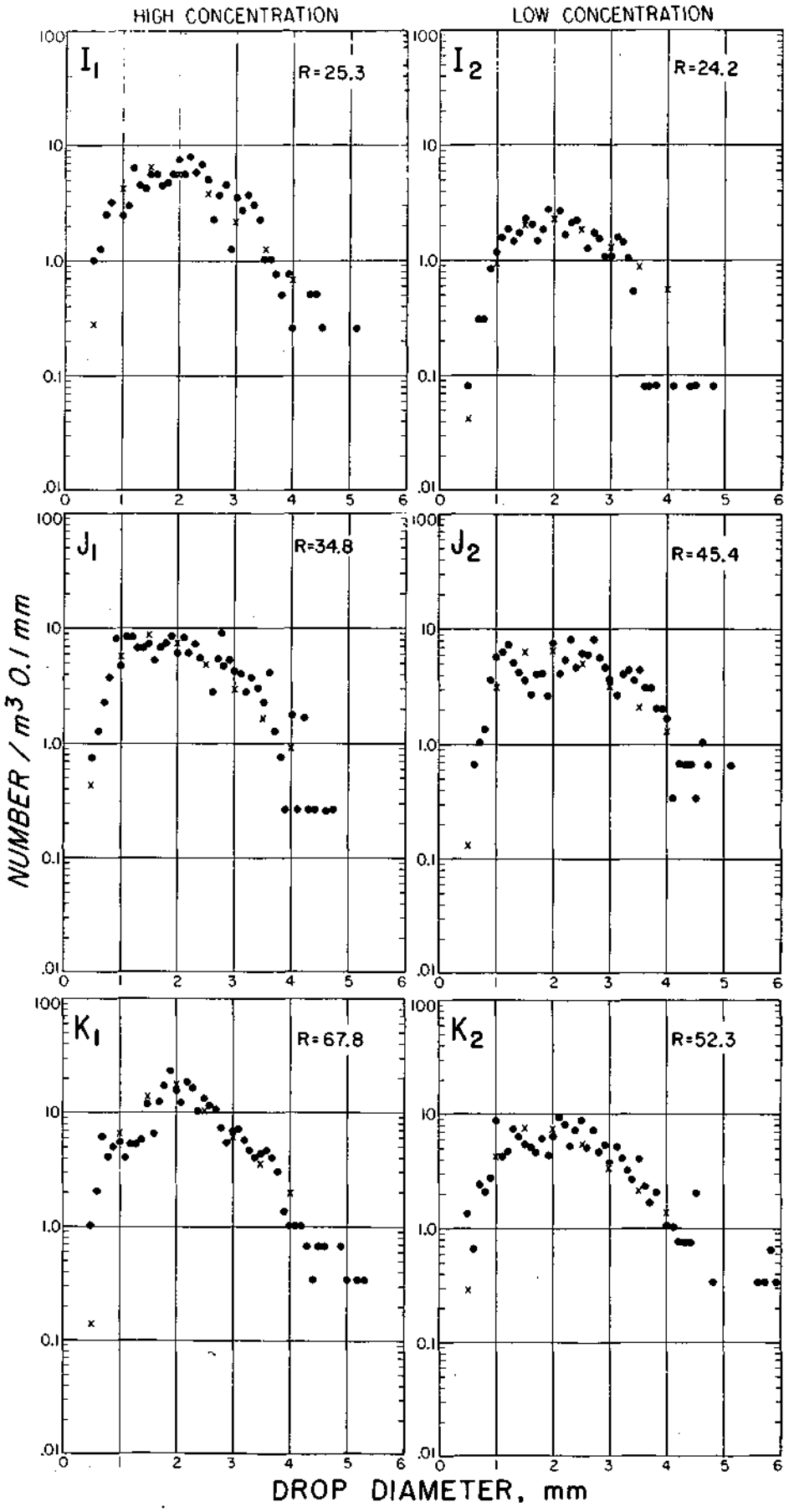

Fig. 6. Average drop-size distributions for the low and high concentration cases at Flagstaff, Arizona.

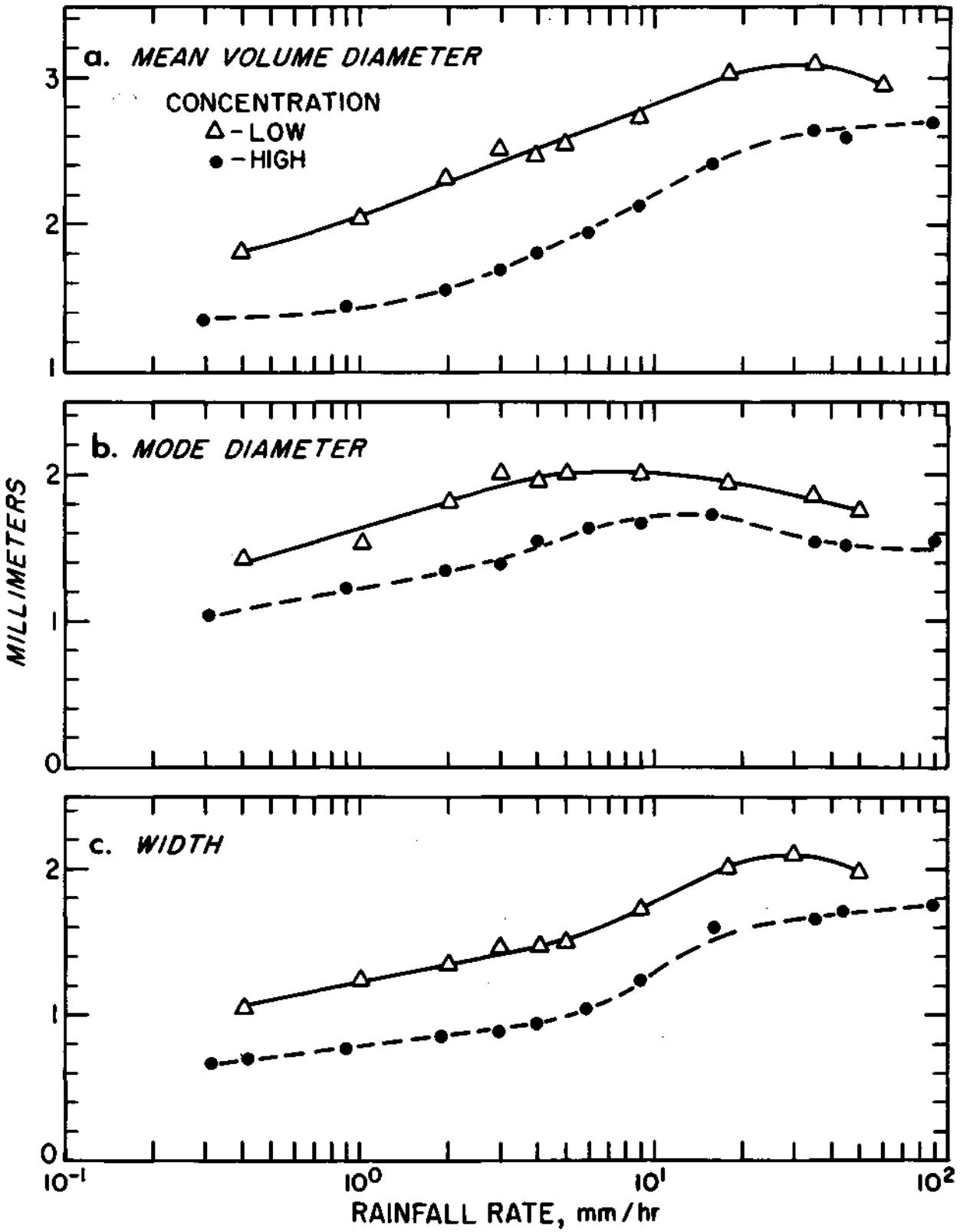

Fig. 7. Comparison of raindrop spectra parameters with rainfall rate for low and high concentration cases.

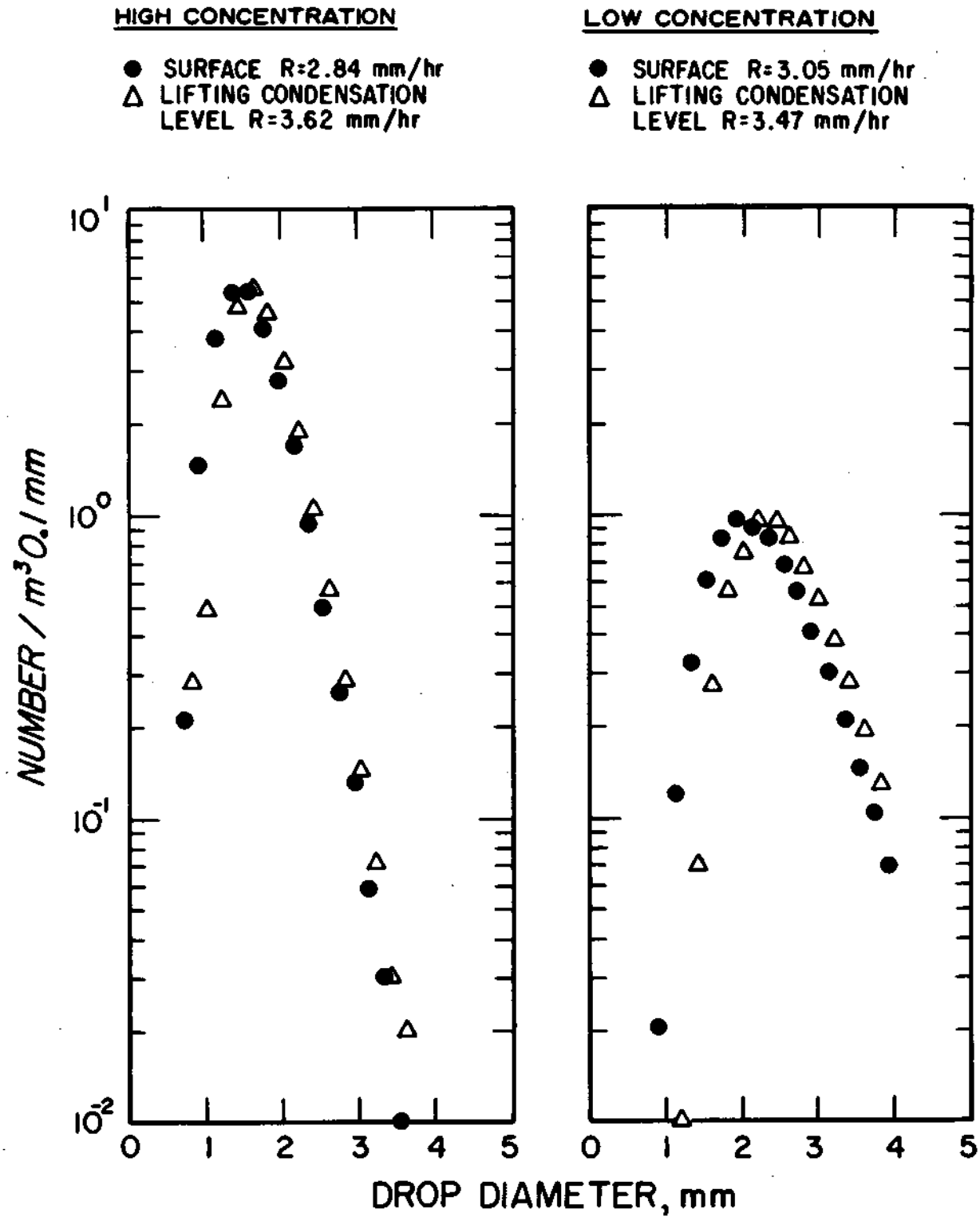

Fig. 8. Evaporation effects for the high and low concentration cases.

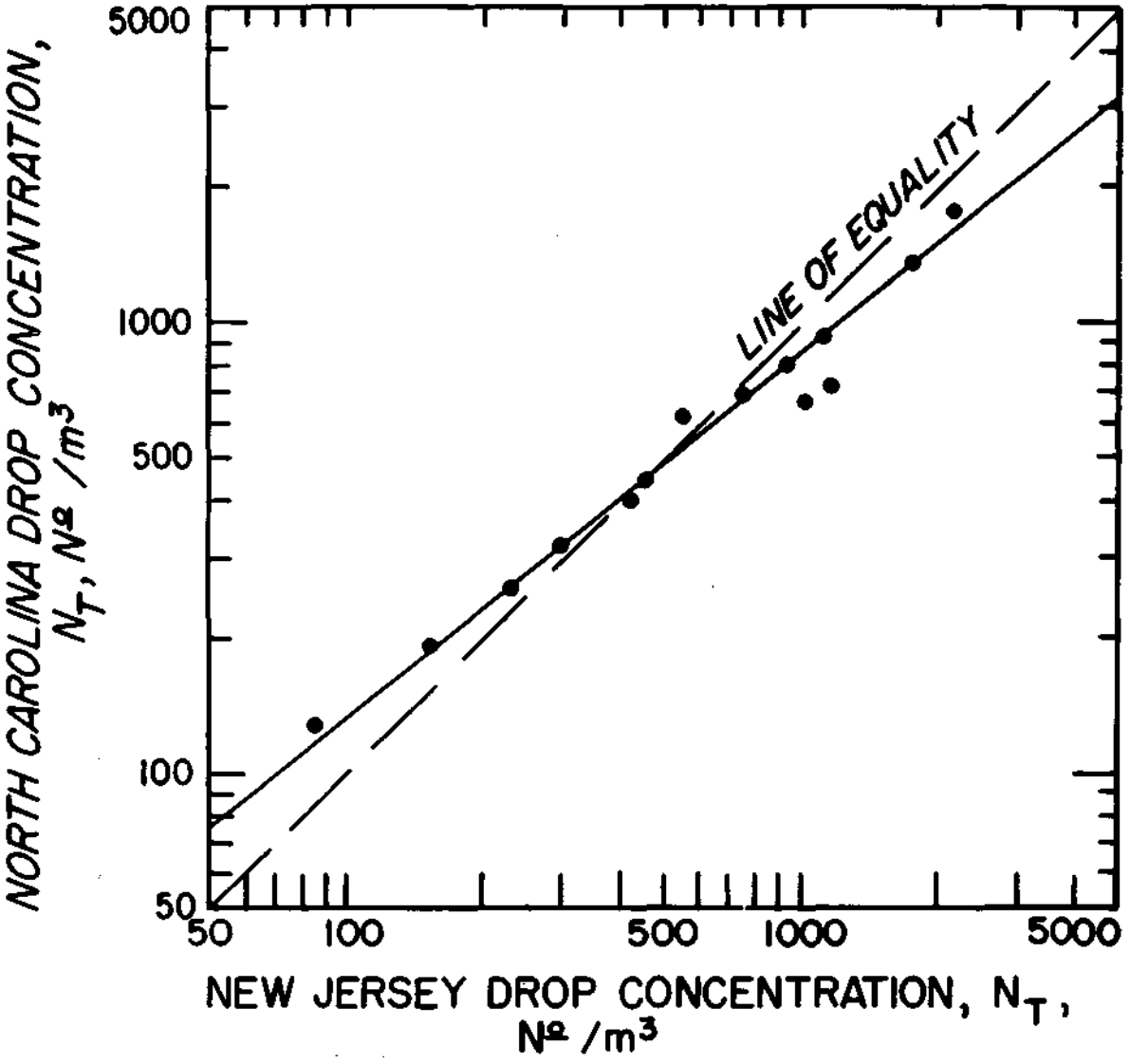

Fig. 9. Drop concentrations for Island Beach, New Jersey and Coweeta, North Carolina (from average spectra for all data, no stratification).

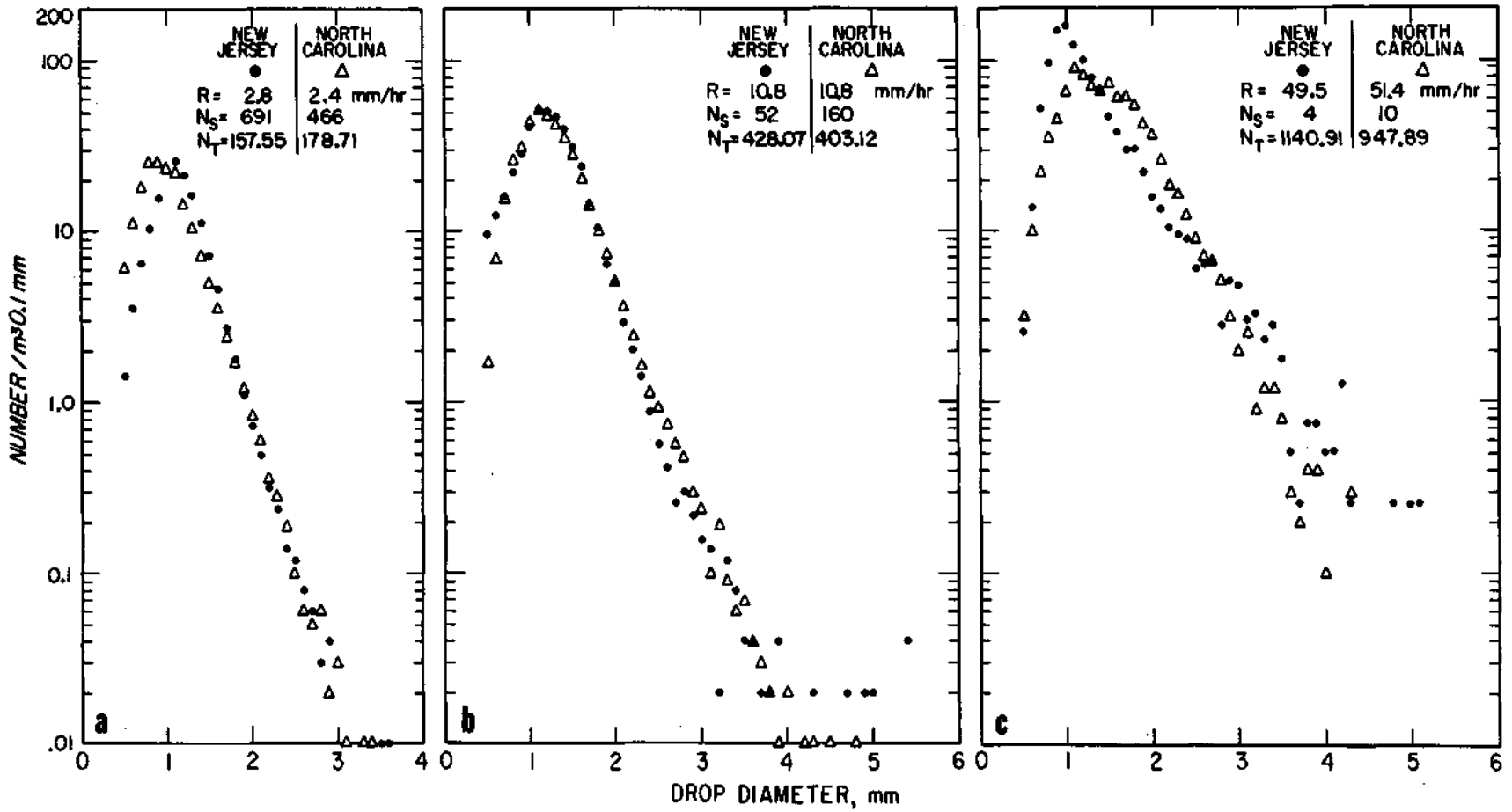

Fig. 10. Raindrop spectra from New Jersey and North Carolina.

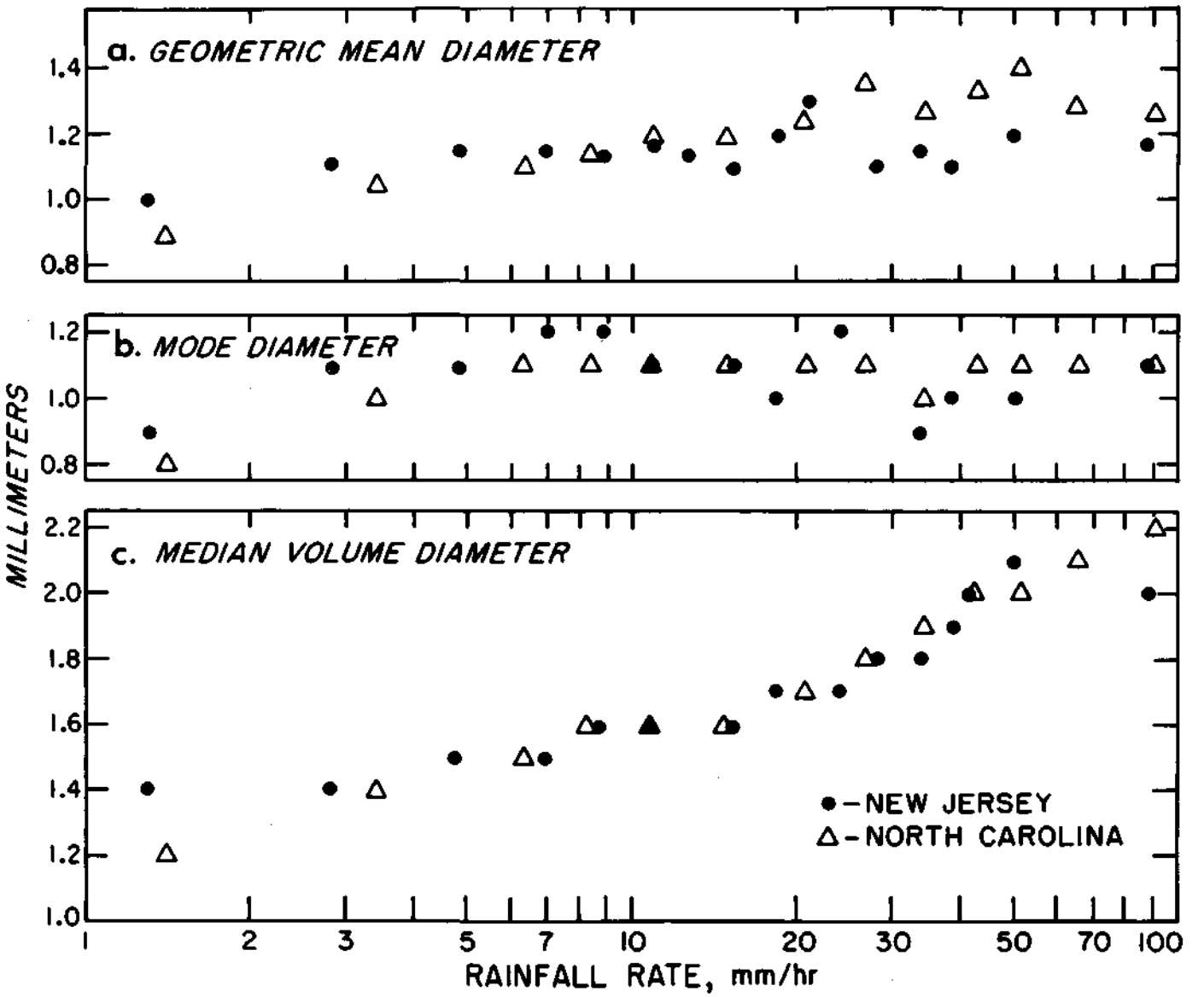

Fig. 11 Raindrop spectra parameters as a function of rainfall rate for New Jersey and North Carolina average drop-size spectra.

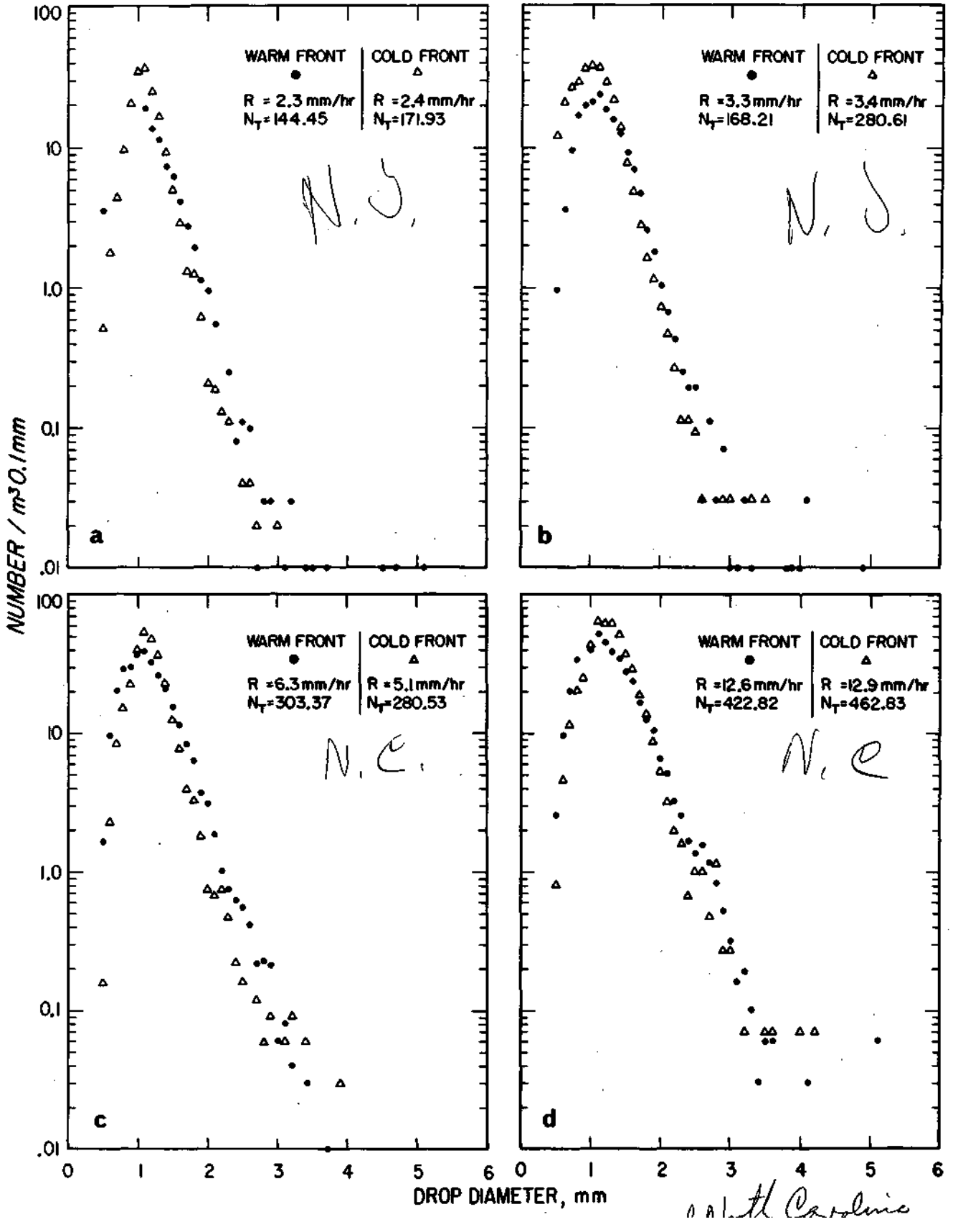

Fig. 12. Raindrop spectra from New Jersey for cold front and warm front synoptic classifications.

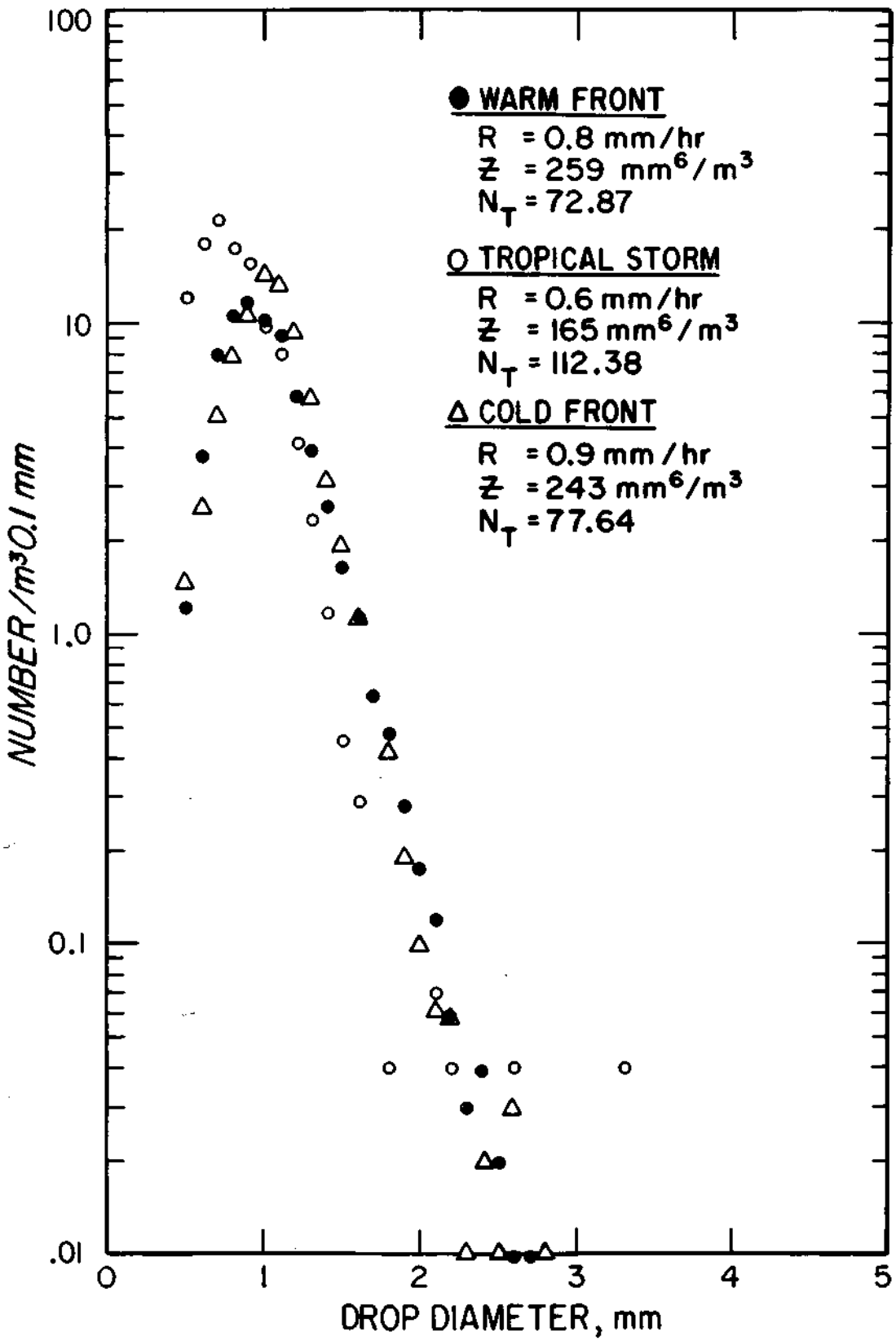

Fig. 13. Raindrop spectra from New Jersey for cold front, warm front, and tropical storm classifications.

APPENDIX A

A COMPARISON OF RAINDROP SIZE SPECTRA BETWEEN MIAMI, FLORIDA, AND CORVALLIS, OREGON*

Robert Cataneo

Illinois State Water Survey-

Abstract

Corvallis, Oregon, and Miami, Florida, two locations where raindrop data have been collected using the raindrop camera, a device which photographs raindrops as they fall, have been compared with respect to the raindrop spectra that have been determined with the camera. The spectra were contrasted with respect to total number of drops (N_T) per average rain rate, per cubic meter of sample, geometric mean diameter (D_G), which is associated with a log-normal distribution, mode diameter (D_M), and the diameter of drops at which half the liquid water content lies above that diameter and half below (D_L). Results indicate that, for similar rainfall rates, Corvallis, Oregon has more of the relatively small drops as well as more of the relatively large ones, than Miami, Florida. As a consequence of this, it is found that greater radar reflectivities exist at Corvallis than at Miami for the same or similar rainfall rates.

Introduction

Much data have been collected with the raindrop camera, as described by Jones and Dean (1953) and Mueller (1960). These data include drop-size distributions for rains in several climatic regions throughout the world, and were obtained in an attempt to establish relationships between radar reflectivity and rainfall rate for these regions.

In the following discussion, a drop-size distribution is characterized by the number of drops in each 0.1 mm size interval from 0.5 mm - 7.9 mm in diameter. To date, all of the analyses have not been completed, although radar-rainfall relationships have been determined for most of the locations. Of course, statements concerning relationships involving rainfall rate (R), and the radar reflectivity factor (Z) must necessarily involve a discussion of the kinds of drop-size distributions that exist during the rains, since Z is directly dependent on D^6, the sixth power of the drop diameters, where:

---

*To be presented at the 60th Annual Meeting of the Illinois State Academy of Science, at Charleston, Illinois, April 28, 1967.

$$Z = \sum_{D=0.5}^{D=7.9} n_D D^6 \qquad (1)$$

n_D being the number of drops of diameter D. If unique distributions existed in nature for various climatic areas, then unique R-Z relationships would follow. Unfortunately, this is not the case. However, an examination of the raindrop-size spectra that do exist would certainly be of interest and value in any attempt to establish R-Z relationships. Two locations where raindrop data were collected, Miami, Florida, and Corvallis, Oregon, have been compared with respect to their drop-size distributions, and the results are presented herein.

Method of Analysis

Briefly, the raindrop camera takes seven pictures, approximately 1-1/2 seconds apart, at the beginning of a minute, and then becomes inactive for the remainder of the minute. Each frame represents a volume of about 1/7 cubic meter, so one minute of data represents approximately one cubic meter. The drops are measured individually, and their number and size are punched onto data cards.

In order to discover general trends and characteristics associated with the distributions, it was necessary to examine average drop-size spectra in the two locations, rather than individual minutes of data. The averages were determined as follows. The data from each of the two locations were sorted in ascending order according to rainfall rate, and then grouped into intervals 1.0 mm/hr wide at the lowest rates, increasing in size at higher rates. The average number of drops per cubic meter in each 0.1 mm increment of drop diameter from 0.5-7.0 mm, along with other related parameters, was calculated by a computer. For this study, all types of rains were grouped together; there was no stratification of the data according to various rain types or synoptic types, for example, since the purpose of this study was to make general comparisons between the two locations.

One method of comparing two groups of distributions is to examine the N_T's for the same or similar rainfall rates from the two locations on log-log coordinates, where N_T is the total number of drops per cubic meter of sample for a particular rain rate. Figure 1 is an example of this where the ordinate represents Oregon, and the abscissa represents Miami. Each point then represents the average total number of drops for each location for the same average rain rate. Now, it is somewhat difficult to point to one parameter and state that it alone, or together with another, describes a particular drop-size spectrum completely, so we should also

examine other factors. In Fig. 2, three comparisons are made between the two areas, on log-log coordinates, with average rainfall rate as abscissa and D_G, D_M and D_L respectively as ordinate. D_M is the diameter of the mode of the spectrum, which is the diameter of the size drop that occurs in the largest numbers. D_G is the geometric mean diameter with:

$$\ln D_G = \frac{\sum_{i=1}^{i=n} n_i \ln D_i}{N_T} \qquad (2)$$

as described in an equation for a log normal distribution fit for the drop-size spectra, and D_L is the median volume diameter which is the diameter of the drop-size where half of the liquid water content of the distribution, for the one cubic meter sample, lies above that drop-size and half below. One should also examine the relationship between N_D and D, as in Fig. 3, where N_D is the number of drops of diameter D. There are other means of comparing spectra, but it is felt that the ones used in this discussion are the most directly related to the distributions.

Results of Analysis

Examination of the N_T comparison between the two locations (Fig. 1) reveals that, for the same rainfall rates, Oregon consistently has more drops than Miami. This would imply that Oregon has smaller drops than Miami, or more specifically, that some average drop-size parameter, such as D_M, D_G or D_L is greater for Miami for the same or similar rainfall rates. In Figs. 2a and 2b this seems to be the case when R is compared with DQ and D_M respectively; both parameters are consistently higher for Miami for the same or similar rainfall rates. However, D_L for Miami is only slightly higher than for Oregon.

To state flatly that Oregon has smaller drops than Miami would not be describing the situation completely; a more detailed examination is necessary. Fig. 3 compares spectra for similar rates from both locations. The particular spectra that were used appear to be representative of their respective areas. These figures indicate that Oregon has more of the smaller size drops, but also more of the larger drops, with a temporary reversal in the vicinity of the Miami mode. This reversal incidentally, is the reason why the rates are the same because, quite obviously, if Oregon had more drops of every size, the rates wouldn't be equal in Fig. 3. Therefore, a more accurate statement concerning the two areas would be that Oregon has both more of the relatively small and relatively large drops, rather than that Oregon has smaller drops.

In addition, an examination of the R-Z relationship from both locations reveals that for equal rainfall rates, Oregon has greater reflectivities. The actual R-Z equations for both regions are as follows; for Oregon,

$$Z = 301\ R^{1.64} \tag{3}$$

for Miami,

$$Z = 286\ R^{1.43} \tag{4}$$

On a plot of R vs Z on log-log coordinates, the linear relationship for Oregon has a greater slope and a greater Z-intercept than Miami. This means that for equal rainfall rates the reflectivities for Oregon are indeed greater. It may be concluded from this, that Oregon has larger drops than Miami, which agrees with the above analyses, although it was found upon examining the actual drop distributions that in addition, Oregon has more of the smaller drops. So apparently, the greater number of larger drops in Oregon represents a sufficient enough difference to result in greater reflectivities, since Z depends directly on D^6, but not large enough to produce greater D_G, D_M and D_L values which are linearly dependent upon D. This agrees with the fact that the N_T's at Oregon are greater than at Miami for the same or similar rates.

It should be pointed out that the number of samples (N_S) used from both areas in Fig. 3 varied substantially, with Miami having four times the number of Oregon in Fig. 3a, and eight times the number in Fig. 3b. There are two reasons for this. First, more data were collected at Miami, and secondly, much of the data taken at Oregon were rains of very low rates; for example, approximately 70 percent were rates of less than 2 mm/hr. It is believed however, that the number of samples taken at Oregon is adequate for a valid comparison. It should also be noted that many of the corresponding N_T's for the relationship in Fig. 1 were arrived at by interpolating between rates on a R-N_T curve in order to obtain the same rainfall rate for both locations when attempting to establish a point on the N_T-N_T curve.

Summary

The drop-size spectra at Oregon and Miami were compared with respect to D_M, D_G, D_L and N_T. The investigation revealed that Oregon rains have larger numbers of drops for the same rainfall rates. Upon closer examination, it was found that the Oregon rains have more of the smaller drops as well as more of the larger ones. The parameters used for the comparison are not necessarily the only ones that are available for valid analyses, but to date appear to be the most appropriate. A similar type of study is underway for the other locations where raindrop-size distribution data have been collected, and the results from those will be available in the near future.

REFERENCES

Jones, D. M. A. and L. A. Dean, 1953. A raindrop camera. Research Report No. 3, U. S. Army Contract No. DA-36-039 SC-42446, Illinois State Water Survey, Urbana, Illinois.

Mueller, E. A., 1960. Study on intensity of surface precipitation using radar instrumentation. Quarterly Technical Report No. 10, U. S. Army Contract No. DA-36-039 SC-75055, Illinois State Water Survey, Urbana, Illinois.

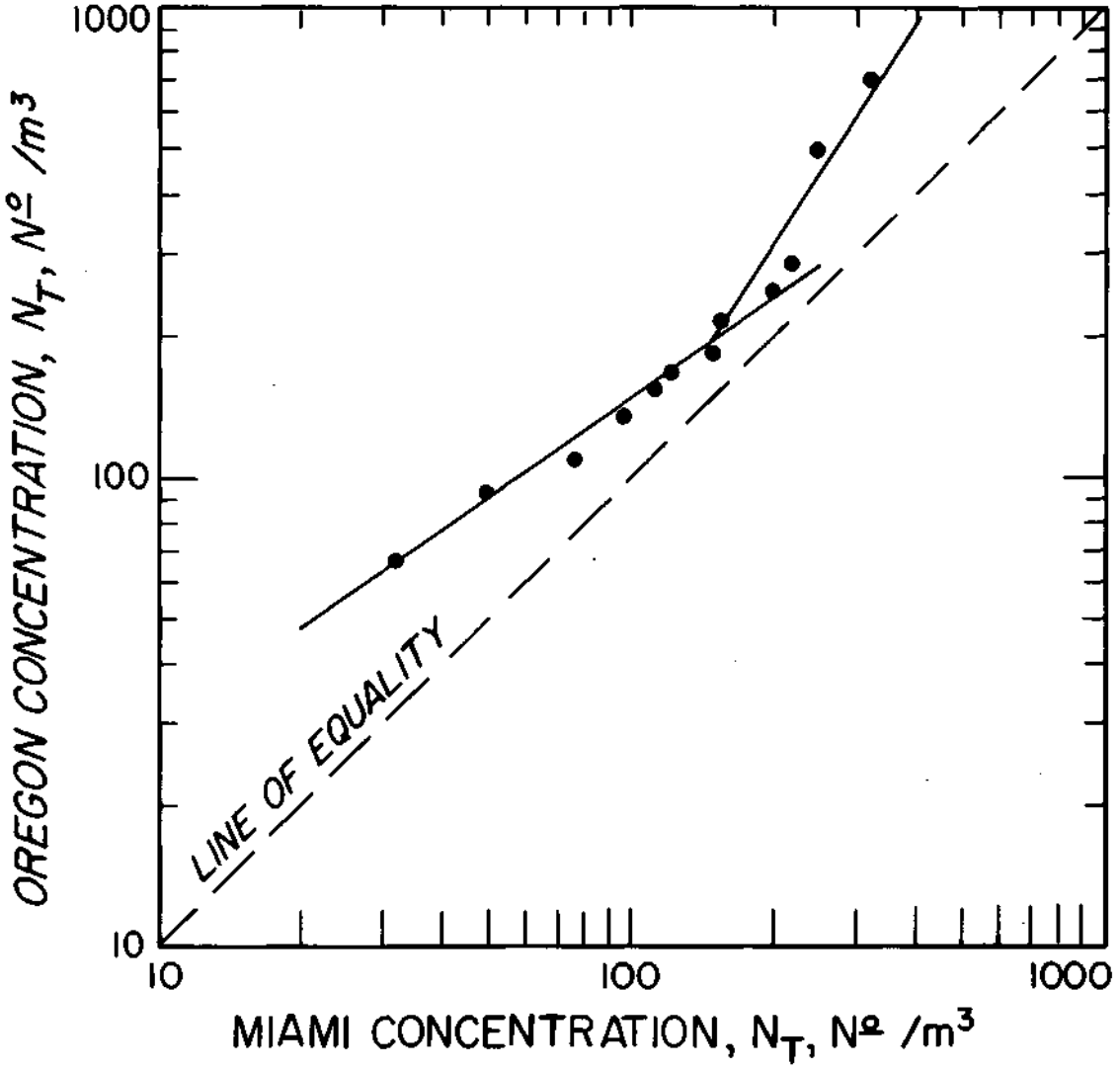

Fig. 1. Drop concentrations for Miami and Oregon (from average spectra for all data, no stratification).

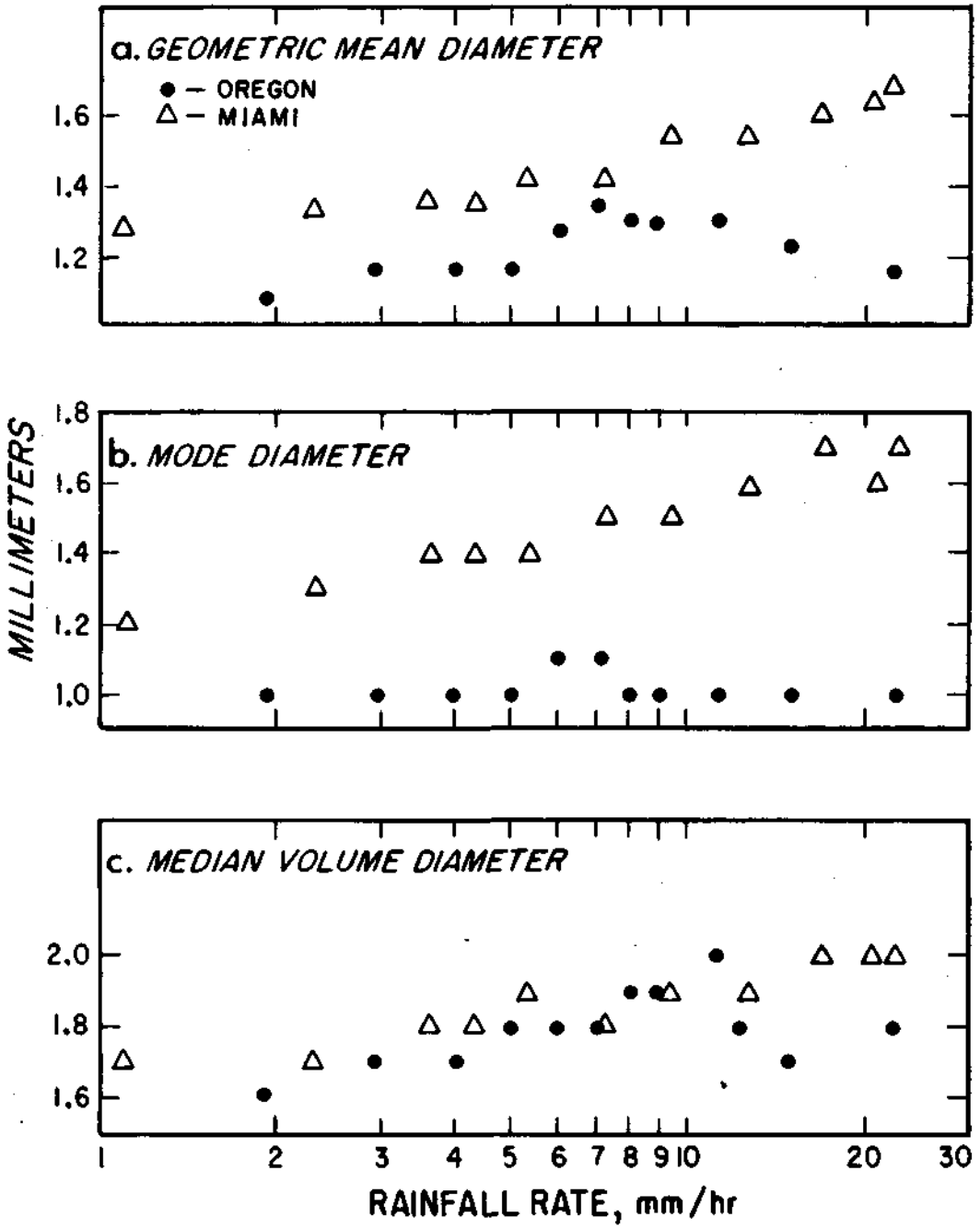

Fig. 2. The mode diameter, the geometric mean diameter, and median volume diameter as a function of rainfall rate for Miami and Oregon.

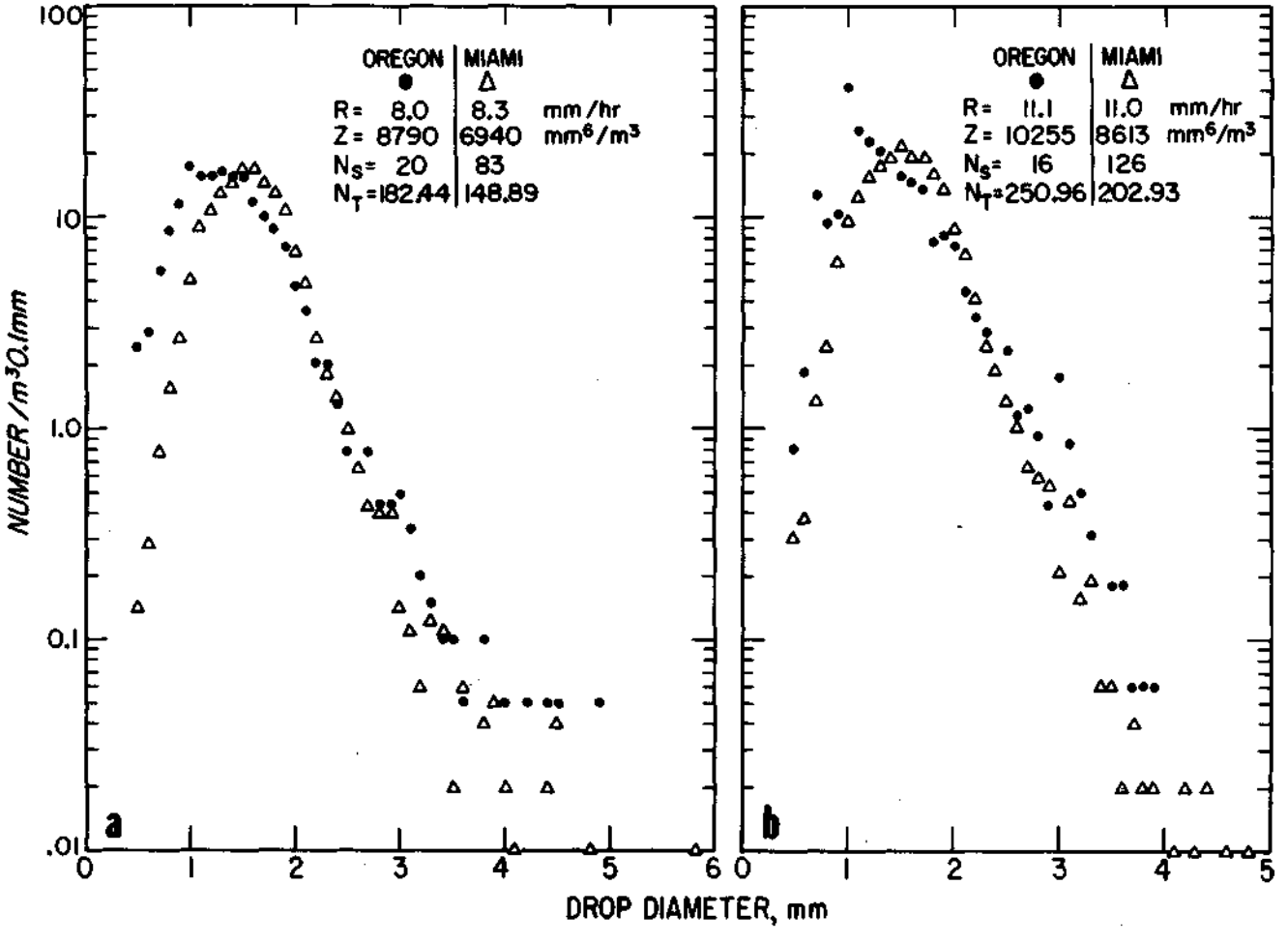

Fig. 3. Raindrop spectra from Miami and Oregon.

DISTRIBUTION LIST

ADDRESSEE	NO. COPIES
Commanding General US Army Materiel Command ATTN: AMCRD-TV Washington, D. C. 20315	1
Chief of Research and Development Dept. of the Army ATTN: CRD Washington, D. C. 20310	1
Commanding General US Army Combat Development Command ATTN: CDCMR-E Ft. Belvoir, Virginia 22060	1
Commanding General US Army CDC Combined Arms Group Ft. Leavenworth, Kansas 66027	1
Commanding General US Army CDC Combat Support Group Ft. Belvoir, Virginia 22060	1
Commanding General US Continental Army Command ATTN: Reconnaissance Br, ODCS for Intelligence Ft. Monroe, Virginia 23351	1
Commanding General US Army Electronics Command ATTN: AMSEL-EW Ft. Monmouth, New Jersey 07703	1
Commanding Officer Fort Detrick ATTN: Environmental Analysis Office Frederick, Maryland 21701	1
Director US Army Engineer Waterways Experiment Station ATTN: WES-FV Vicksburg, Mississippi 39181	1
Chief Atmospheric Sciences Research Div Atmospheric Sciences Laboratory US Army Electronics Command Ft. Huachuca, Arizona 85613	1

ADDRESSEE	NO. COPIES
Chief Atmospheric Sciences Office Atmospheric Sciences Laboratory US Army Electronics Command White Sands Missile Range, New Mexico 88002	1
US Army Munitions Command Operations Research Group Edgewood Arsenal, Maryland 21010	1
Commanding Officer US Army Dugway Proving Ground ATTN: Meteorology Division Dugway, Utah 84022	1
Commanding Officer US Army CDC Artillery Agency Ft. Sill, Oklahoma 73504	1
Commanding Officer US Army CDC Communications Electronics Agency Ft. Monmouth, New Jersey 07703	1
Commanding Officer US Army CDC CBR Agency ATTN: Mr. N. W. Bush Ft. McClellan, Alabama 36205	1
Commanding General US Army Electronics Proving Ground ATTN: Field Test Dept. Ft. Huachuca, Arizona 85613	1
Commanding General Deseret Test Center ATTN: Design and Analysis Div Ft. Douglas, Utah 84113	1
Commandant US Army CBR School, Micrometeorological Section Ft. McClellan, Alabama 36205	1
Ass't Chief of Staff for Intelligence Dept. of the Army ATTN: ACSI-DSRSI Washington, D. C. 20310	1

ADDRESSEE	NO. COPIES
Assistant Chief of Staff for Force CBR Nuclear Operations Directorate Dept. of the Army Washington, D. C. 20310	1
Commander USAF Air Weather Service (MATS) ATTN: AWSSS/TIPD Scott Air Force Base, Illinois 62225	1
Commander Air Force Cambridge Research Laboratories ATTN: CRXL L. G. Hanscom Field Bedford, Massachusetts 01730	1
Chief of Naval Operations, Dept. of the Navy ATTN: Code 427 Washington, D. C. 20305	1
Office of US Naval Weather Service US Naval Air Station Washington, D. C. 20390	1
Officer-in-Charge US Naval Weather Research Facility US Naval Air Station, Bldg R-28 Norfolk, Virginia 23511	1
Director, Atmospheric Sciences Program National Sciences Foundation Washington, D. C. 20550	1
Chief, Domestic Section, RD-52.1 Coordination Br Dept. of Transportation, Federal Aviation Administration Washington, D. C. 20580	1
Chief, Fallout Studies Branch Division of Biology and Medicine, Atomic Energy Commission Washington, D. C. 20545	1
Director of Meteorological Systems Office of Applications (FM) National Aeronautics and Space Administration Washington, D. C. 20546	1

ADDRESSEE	NO. COPIES
R. A. Taft Sanitary Engineering Center Public Health Service 4676 Columbia Parkway Cincinnati, Ohio 45202	1
Director, Atmospheric Physics and Chemistry Laboratory Environmental Science Services Administration Boulder, Colorado 80302	1
Defense Documentation Center Cameron Station Alexandria, Virginia 22314	20
National Center for Atmospheric Research ATTN: Library Boulder, Colorado 80302	1
US Dept. of Agriculture, Forest Service Station Lake States Forest Experiment Station, ATTN: E. P. Van Aradel St. Paul Campus, University of Minnesota St. Paul, Minnesota 35101	1
Director, US Naval Research Laboratory ATTN: Code 2027 Washington, D. C.	1
Officer-in-Charge, Meteorological Curriculum US Naval Weather Research Facility, US Naval Air Station, Bldg B48 Norfolk, Virginia 23511	1
The American Meteorological Society Abstracts and Bibliography, ATTN: Mr. M. Rigby P.O. Box 1736 Washington, D„ C.	1
Library, US Weather Bureau Environmental Science Services Administration ATTN: #533 Washington, D. C.	1
Climatic Center, US Air Force Annex 2, 225 D Street, SE Washington, D. C.	1
Dr. Max Nagel, NASA-NRC 30 Memorial Drive Cambridge, Massachusetts	1

ADDRESSEE	NO. COPIES
Meteorology Dept. Florida State University Tallahassee, Florida	1
Meteorology Dept. University of Chicago Chicago, Illinois	1
Dept. of Meteorology and Oceanography N. Y. University, College of Engineering University Heights, Nev ; York 10053	1
Dept. of Meteorology Penn State University, Mineral Industries Bldg. University Park, Pa. 16802	1
Institute of Atmospheric Physics University of Arizona Tucson, Arizona	1
Dr. H. Lettau U. of Wisconsin, Dept. of Meteorology Madison, Wisconsin	1
Commanding General US Army Electronics Command ATTN: AMSEL-RD-MAF Ft. Monmouth, New Jersey 07703	1
Commanding General US Army Electronics Command ATTN: AMSEL-IO-T Ft. Monmouth, New Jersey 07703	1
Commanding General US Army Electronics Command ATTN: AMSEL-BL-AP Ft. Monmouth, New Jersey 07703	6
Director, National Weather Records Center ATTN: Mr. Haggard, Arcade Bldg. Asheville, North Carolina	1
Brookhaven National Laboratories Meteorological Dept. Camp Upton, New York	1
Dr. Pauline Austin Research, Dept. of Meteorology Massachusetts Institute of Technology Cambridge, Massachusetts 02139	1

ADDRESSEE	NO. COPIES
Climatic Center, US Air Force *ANNEX* 2 225 D. Street, SE Washington, D. C,	1
Director, Atmospheric Sciences Program National Science Foundation Washington, D. C.	1
Commanding Officer US Army Research and Development Group (Europe) ATTN: CRD-AF APO New York 09757	1
Commander, US Army Research Office (Durham) Box CM-Duke Station Durham, North Carolina 27706	1
Electronic Systems Div (AFSC), Scientific and Technical Info Div (E STI) L. G. Hanscom Field Bedford, Massachusetts 01731	1
Oregon State University ATTN: Meteorological Dept, Dr. Decker Corvallis, Oregon	1
Dr. Edwin Kessler, Director, National Severe Storms Laboratory US Weather Bureau 1616 Holley Avenue Norman, Oklahoma	1
Dept. of Meteorology, University of Miami P.O. Box 8003 ATTN: Mr. Homer Hiser Coral Gables, Florida 33124	1

Security Classification

DOCUMENT CONTROL DATA - R & D

(Security classification of title, body of abstract and indexing annotation must be entered when the overall report is classified)

1. ORIGINATING ACTIVITY (Corporate author) Illinois State Water Survey University of Illinois Urbana, Illinois 61801	2a. REPORT SECURITY CLASSIFICATION Unclassified 2b. GROUP n/a

3. REPORT TITLE

Investigation of the Quantitative Determination of Precipitation by Radar.

4. DESCRIPTIVE NOTES (Type of report and inclusive dates)

Interim Report No. 1, 1 Oct 66 - 31 Mar 67.

5. AUTHOR(S) (First name, middle initial, last name)

E. A. Mueller, A. L. Sims, and R. Cataneo

6. REPORT DATE	7a. TOTAL NO. OF PAGES	7b. NO. OF REFS
June 1967	52	9

8a. CONTRACT OR GRANT NO.	9a. ORIGINATOR'S REPORT NUMBER(S)
Contract DA28-043 AMC-02071(E) b. PROJECT NO. 1V0-14501-B-53A-07 c. d.	9b. OTHER REPORT NO(S) (Any other numbers that may be assigned this report) Technical Report ECOM-02071-1

10. DISTRIBUTION STATEMENT

Distribution of this report is unlimited.

11. SUPPLEMENTARY NOTES	12. SPONSORING MILITARY ACTIVITY
None.	US Army Electronics Command AMSEL-BL-AP Fort Monmouth, New Jersey

13. ABSTRACT

The results of a study of the measurement of rainfall by radar at a range of 75 miles are presented,, Some of the problems of radar measurements at this range are found to be attenuation and effects of the radar beam's vertical extent at distant ranges.

The analysis of drop-size data from rains at Flagstaff, Arizona shows that the radar-rainfall relationships there are quite different from those measured elsewhere by the drop camera technique.

Results of a study of drop-size distributions from New Jersey and North Carolina are presented. In many respects, the data from these two locations are similar.

A paper dealing with the analysis of drop-size data from Florida and Oregon is included as an appendix.

DD FORM 1 NOV 65 1473 REPLACES DD FORM 1473, 1 JAN 64, WHICH IS OBSOLETE FOR ARMY USE.

Security Classification

14. KEY WORDS	LINK A		LINK B		LINK C	
	ROLE	WT	ROLE	WT	ROLE	WT
meteorology						
weather radar						
precipitation						
raindrop size distribution						
rainfall rate						

INSTRUCTIONS

1. ORIGINATING ACTIVITY: Enter the name and address of the contractor, subcontractor, grantee, Department of Defense activity or other organization *(corporate author)* issuing the report.

2a. REPORT SECURITY CLASSIFICATION: Enter the overall security classification of the report. Indicate whether "Restricted Data" is included. Marking is to be in accordance with appropriate security regulations.

26. GROUP: Automatic downgrading is specified in DoD Directive 5200.10 and Armed Forces Industrial Manual. Enter the group number. Also, when applicable, show that optional markings have been used for Group 3 and Group 4 as authorized.

3. REPORT TITLE: Enter the complete report title in all capital letters. Titles in all cases should be unclassified. If a meaningful title cannot be selected without classification, show title classification in all capitals in parenthesis immediately following the title.

4. DESCRIPTIVE NOTES: If appropriate, enter the type of report, e.g., interim, progress, summary, annual, or final. Give the inclusive dates when a specific reporting period is covered.

5. AUTHOR(S): Enter the name(s) of author(s) as shown on or in the report. Enter last name, first name, middle initial. If military, show rank and branch of service. The name of the principal author is an absolute minimum requirement.

6. REPORT DATE: Enter the date of the report as day, month, year; or month, year. If more than one date appears on the report, use date of publication.

la. TOTAL NUMBER OF PAGES: The total page count should follow normal pagination procedures, i.e., enter the number of pages containing information.

lb. NUMBER OF REFERENCES: Enter the total number of references cited in the report.

8a. CONTRACT OR GRANT NUMBER: If appropriate, enter the applicable number of the contract or grant under which the report was written.

8*b*, 8c, & 8*d*. PROJECT NUMBER: Enter the appropriate military department identification, such as project number, subproject number, system numbers, task number, etc.

9a. ORIGINATOR'S REPORT NUMBER(S): Enter the official report number by which the document will be identified and controlled by the originating activity. This number must be unique to this report.

96. OTHER REPORT NUMBER(S): If the report has been assigned any other report numbers *(either by the originator or by the sponsor),* also enter this number(s).

10. AVAILABILITY/LIMITATION NOTICES: Enter any limitations on further dissemination of the report, other than those imposed by security classification, using standard statements such as:

(1) "Qualified requesters may obtain copies of this report from DDC ."

(2) "Foreign announcement and dissemination of this report by DDC is not authorized."

(3) "U. S. Government agencies may obtain copies of this report directly from DDC. Other qualified DDC users shall request through _____."

(4) "U. S. military agencies may obtain copies of this report directly from DDC Other qualified users shall request through _____."

(5) "AH distribution of this report is controlled. Qualified DDC users shall request through _____."

If the report has been furnished to the Office of Technical Services, Department of Commerce, for sale to the public, indicate this fact and enter the price, if known.

11. SUPPLEMENTARY NOTES: Use for additional explanatory notes.

12. SPONSORING MILITARY ACTIVITY: Enter the name of the departmental project office or laboratory sponsoring *(paying for)* the research and development. Include address.

13. ABSTRACT: Enter an abstract giving a brief and factual summary of the document indicative of the report, even though it may also appear elsewhere in the body of the technical report. If additional space is required, a continuation sheet shall be attached.

It is highly desirable that the abstract of classified reports be unclassified. Each paragraph of the abstract shall end with an indication of the military security classification of the information in the paragraph, represented as *(TS), (S). (C). or (U).*

There is no limitation on the length of the abstract. However, the suggested length is from 150 to 225 words.

14. KEY WORDS: Key words are technically meaningful terms or short phrases that characterize a report and may be used as index entries for cataloging the report. Key words must be selected so that no security classification is required. Idenfiers, such as equipment model designation, trade name, military project code name, geographic location, may be used as key words but will bo followed by an indication of technical context. The assignment of links, rules, and weights is optional.